Eng. Sci., 2024, **30**, 1116

Engineered Science
DOI: https://dx.doi.org/10.30919/es1116

Microwave Imaging for Breast Cancer Detection- A Comprehensive Review

Deepshikha Bhargava,[1] Phadungsak Rattanadecho[2,*] and Krit Jiamjiroch[2]

Abstract

The paper presents an extensive discussion on Microwave Imaging (MI) for breast cancer detection. Breast cancer has become a major cause of death among women worldwide, this makes the early detection of the cancerous tumor very essential in providing a rapid and effective treatment. Microwave Breast Imaging (MBI) is an emerging technique that is non-ionizing, non-invasive, safer and cheaper in comparison to the conventional techniques. It uses microwave radiation to generate an internal image of the breast, showing the tumor embedded in the breast layers. The paper begins by introducing the basic working principles of MBI and its types, anatomy of the breast, and the differences in the dielectric properties between normal and malignant tissues. Active type of MBI – tomography and radar-based imaging are mainly covered in this paper. The most important part of active microwave imaging, i.e. antennas used for scanning the breast are also discussed. Moreover, numerical, experimental as well as clinical studies performed over the years are highlighted. In the end, challenges in the current techniques and future prospective of MBI are presented. Overall, this review paper provides a comprehensive insight into the techniques used in MBI, and the state-of-the-art research in this field.

Keywords: Breast cancer; Microwave breast imaging (MBI); Antennas; Tomography imaging, Radar-based imaging.
Received: 01 July 2023; Revised: 17 February 2024; Accepted: 25 February 2024.
Article type: Review article.

1. Introduction

According to World Health Organization (WHO) breast cancer has become the most common cause of death among women worldwide. In 2020, there were 2.3 million women diagnosed with breast cancer and 685000 deaths. It has been predicted that by 2040 there will be 3 million cases of breast cancer per year and 1 million deaths per year. In such scenario, early detection of breast cancer becomes essential for providing an effective treatment and increasing the overall survival rate. An early detection of breast cancer can increase the five-year survival rate to up to 90%.[1,2] For this reason, researchers have been actively seeking a screening method that exhibits the following qualities-

(a) Minimizes patients' discomfort during the screening process.
(b) Produces high resolution images of the breast and tumor.
(c) Cost-effective and easy access universally.
(d) Ensures the safety of patients during extended use of screening methods.
(e) Ability to differentiate between malignant, benign, and cancerous tumors.

WHO has recommended that women above the age of 50 should go for breast screening every two years, and women with breast cancer history even earlier. Awareness regarding the breast cancer has been taken seriously and self-examination is also promoted at areas where the hospitals cannot provide screening tests. The most popular screening methods introduced for breast cancer over the years are X-ray mammography, Ultrasound, and MRI. X-ray Mammography has been the gold standard for breast cancer imaging. It generates 2D images of the breast and is used frequently at the early stages of screening. However, it uses ionizing radiation that cannot be used to irradiate human

[1] *Department of Mechanical Engineering, Faculty of Engineering, Kasetsart University, 50 Ngam Wong Wan Road, Ladyaow Chatuchak, Bangkok 10900, Thailand.*
[2] *Center of Excellence in Electromagnetic Energy Utilization in Engineering (CEEE), Department of Mechanical Engineering, Faculty of Engineering, Thammasat University (Rangsit Campus), 99 moo 18, Klong Luang, Pathum Thani 12120, Thailand.*
*Email: ratphadu@engr.tu.ac.th (P. Rattanadecho)

tissues for extended periods due to its health concerns. X-ray mammography can also be uncomfortable for women as it requires the breast to be compressed between the mammography plates, shown in Fig. 1.[3] It is also not suitable in cases of dense breasts because the mammograms of both dense breast and tumor often appears white. Moreover, X-ray mammography has also been showing false negative and false positive results in tumor detection, making it a less reliable method for breast cancer imaging. Tomosynthesis is another technique similar to X-ray mammography, except that it generates 3D images of the breast, which aids in more comprehensive analysis. However, the X-rays used in this method raise concerns about safety, and the procedure itself can be uncomfortable for women similar to the X-ray mammography.[4,5]

The ultrasound and MRI methods for breast cancer imaging are safer than the X-ray mammography as they use non-ionizing radiation. However, both of these techniques are often not recommended at the early stages of screening. Ultrasound generates low resolution images making it difficult to distinguish between healthy and cancerous tissues. MRI is able to generate high resolution images but it is very expensive and often not suggested as an early-stage screening method for breast cancer. Hence, these methods are mostly used at the later stages of the screening. All of these disadvantages in the current screening methods have led researchers to continue their quest for an alternative technique.[6-8]

A significant difference has been found in the dielectric properties of a healthy and cancerous breast tissue at microwave frequencies. This fact has attracted researchers' interest in using microwave radiation for breast cancer detection. Microwave radiation lies in the non-ionizing radiation region of the EM spectrum, ranging from 300 MHz to 300 GHz. Microwave imaging is a technique that uses microwave radiation to detect the embedded tumor in the breast layers by producing an internal image of the breast. Since microwave imaging uses microwave radiation it is much safer than the X-rays used in the X-ray mammography technique.

Microwave imaging is a non-invasive technique that helps produce the internal image of the breast. It is also safer, cheaper and more comfortable than other available techniques. MI has been widely studied by many researchers and is found to have the potential to detect tumors at an early stage of the screening.[9,10] It is mainly divided into three categories- passive, active, and hybrid microwave imaging, as shown in Fig. 2. Passive microwave imaging uses the thermal radiation emitted by both healthy and unhealthy tissues to identify cancerous tissue within the breast. The cancerous tissues typically have slightly higher temperature than the normal tissues, forming the basis for the passive microwave imaging.[11] In active microwave imaging, microwave signals are transmitted on the breast and the reflected signals after interaction with the breast tissues are recorded. The recorded signals are then processed using algorithms to detect the embedded tumor in the breast.[12,13] Hybrid microwave imaging, as the name suggests, is a mix of both passive and active microwave imaging. It uses both the thermal radiation emitted by the breast tissue and the recorded reflected signals to identify the embedded tumor in the breast.[14,15] In this review paper we are going to focus on the active type of microwave imaging- tomography and radar-based, as this type of microwave imaging provides targeted examination and is preferred for early-stage detection.

In a typical microwave imaging system, a transmitter is used to generate microwaves and a receiver is used to record the reflected waves. Breast tissues are irradiated by a transmitter, where the microwaves travel through the breast tissues having different dielectric properties. As the microwaves interact with the tissues some part of the waves gets absorbed by the tissues whereas some of it gets scattered/reflected. The reflected waves are recorded by the receiver, and with the help of an imaging algorithm, an image of the breast is generated, showing the tumor embedded in the breast tissues.[16]

One of the most important parts of active microwave imaging is the antenna used to transmit and receive the signals. Over the years different MBI systems have been proposed with different types and numbers of antennas. Fig. 3 shows a setup of MI system for breast cancer detection. The setup consists of - a table (where the patient lies in a prone position), an antenna sensor bowl (where the breast is suspended), a network analyzer, and a computer for data processing. The antenna sensor scans the breast without any breast compression, the data is collected and processed, and an image of the breast is generated.

In tomography microwave imaging, a dielectric profile of the whole breast is created using an ill-posed advanced algorithm. Meanwhile, radar-based microwave imaging generates a 2D image of the breast containing the tumor. Detailed and up-to-date research covering the numerical, experimental, and clinical studies in active microwave imaging is discussed in this paper.[17-19]

In the literature, there are several review papers on MBI. Alsawaftah *et al.*[8] and Benny *et al.*[20] presented a review paper discussing all three types of MBI techniques and the dielectric properties of the tissues. Kwon *et al.*[3] in their review paper discussed the active MBI technique and the dielectric properties of the tissues. Aldhaeebi *et al.*[13] discussed only the active MBI techniques. Borja *et al.*,[21] Rafique *et al.*,[22] and Misilmani *et al.*[23] presented a survey on the different types of the antenna used in biomedical imaging applications. Recently, Wang *et al.*[24] presented a detailed review paper on MBI, which included the active MBI techniques and dielectric properties of the tissues. To our knowledge there has been a lack of a single key paper that covers all the important aspects of an active MBI system, such as – breast and tumor anatomy, dielectric properties, antennas used in the MBI, and the type of MBI technique itself. Hence, compared to the available literature, in this review paper we are trying to provide a key/reference paper for the researchers interested in this field by including the up-to-date simulation, experimental, and clinical studies performed in the field of MBI. The paper is organized as follows: Section 2 discusses the anatomy of the breast and tumor, and how the dielectric properties of a healthy and cancerous tissues differ from each other. In section 3, different types of antennas and their usage in MBI are discussed. Later in section 4 & 5 research done in tomography and radar-based MBI is discussed. Section 6 talks about the clinical trials, challenges, and future work. Lastly section 7 concludes the paper and discusses the future perspectives of active MBI.

2. Breast anatomy and dielectric properties

Figure 4 shows the anatomy of a healthy breast. It is a glandular organ composed of mammary glands, ducts, fibrous tissue and fatty tissues. The mammary glands are small sacs made of lobular tissues that produce milk. The ducts are tube-like structures that carry this milk from the lobular tissue to the nipple. Both the lobular and ducts make a web like structure throughout the breast. The fibrous tissue acts as a connective tissue, providing shape and support for the glandular tissues. Whereas the fatty tissues fill the space between the ducts, fibrous tissues, and other connective tissues in the breast. The amount of fatty tissues in the breast depends on the female's age, weight, and genetics. Although, malignant tumors can form anywhere throughout the breast, they are more often seen to develop in the ducts and lobules tissues. Breast cancer types are mainly classified into four categories- Ductal carcinoma in situ (DCIS), Invasive ductal carcinoma (IDC), Lobular carcinoma in situ (LCIS), and Invasive lobular carcinoma (ILC). "In situ" refers to the cancer cells in the breast that have not yet spread to the surrounding tissues, whereas, "invasive" refers to cancer cells that have spread into the nearby tissues. Fig. 5 shows the breast cancer in the ducts (DCIS and IDC)

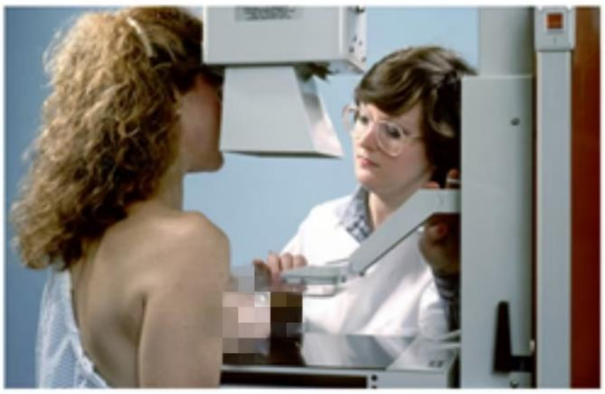

Fig. 1 Screening methods for MBI: X-ray mammography. Reproduced with the permission form [25].

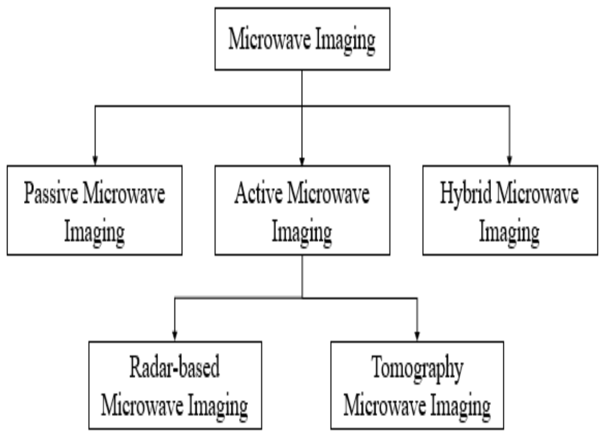

Fig. 2 Types of Microwave Imaging.

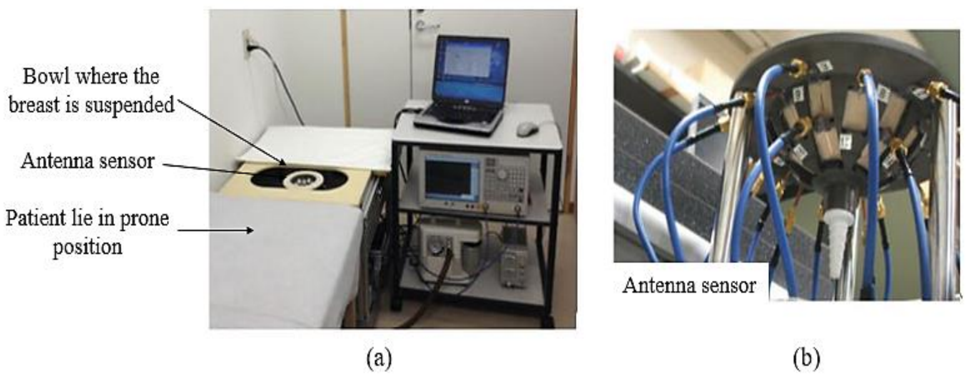

Fig. 3 (a) Microwave Breast imaging setup, and (b) antenna sensor. Reproduced with the permission from [26].

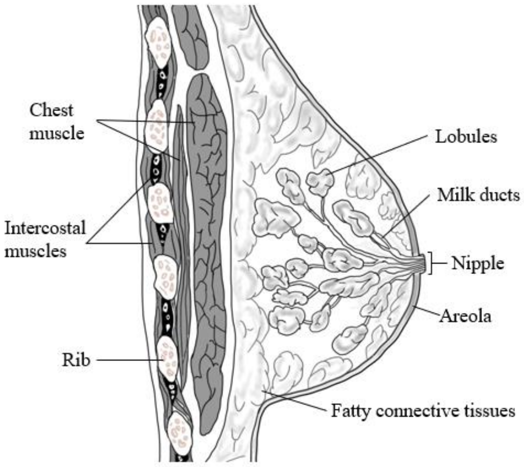

Fig. 4 Anatomy of a healthy breast.

and Fig. 6 shows the breast cancer in the lobules (LCIS and ILC). Figs. 5(a) and 6(a) show the healthy cells of ducts and lobules, respectively. Figs. 5(b) and 6(b) show that cancer cells developed non-invasively in the ducts and lobules. Figs. 5(c) and 6(c) show the cancer cells spreading out of the ducts and lobules, respectively, becoming the invasive type of cancer.[27]

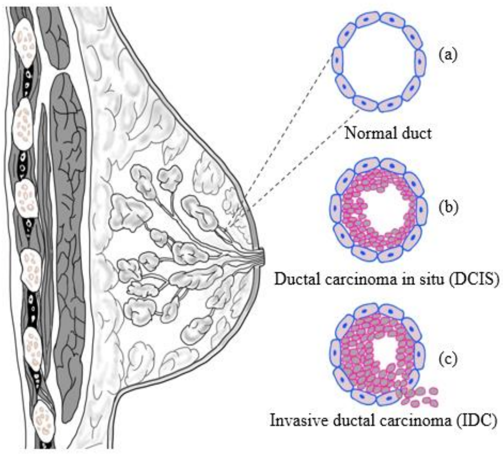

Fig. 5 Ductal carcinoma cancer.

The Backbone of microwave breast imaging is the significant difference found between the dielectric properties of a healthy and malignant tissue at microwave frequencies. Malignant tissues have higher values of dielectric properties (electrical conductivity and permittivity) than the healthy tissues (such as fat). This is because malignant tissues are rich in water content, and tissues with high-water content have higher value of dielectric properties.

Dielectric properties of tissues basically give away the information on how that tissue would react to a specific frequency after upon interaction. The relative dielectric permittivity ε is expressed in Eq. 1 as-[9,28]

$$\varepsilon(\omega) = \varepsilon' - j\varepsilon''(\omega) \quad (1)$$

where j = $\sqrt{-1}$, ω is the angular frequency, ε' is the dielectric constant and $\varepsilon''(\omega)$ is the loss factor. The dielectric constant (ε') determines the material's ability to store energy and the loss factor ($\varepsilon''(\omega)$) reflects how much that energy is converted into heat and dissipated in the material.

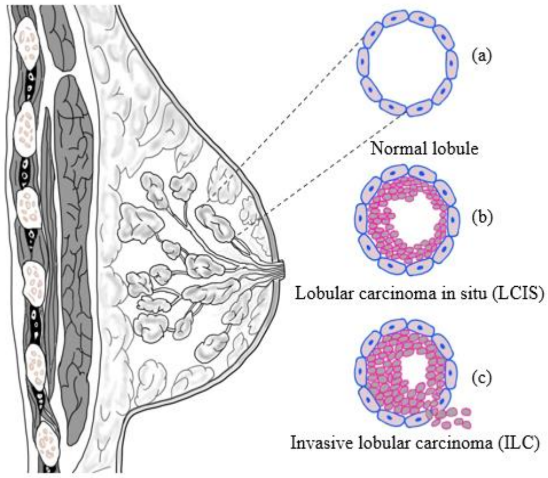

Fig. 6 Lobular carcinoma cancer.

The dielectric conductivity of the tissues is expressed in Eq. 2 as:[28]

$$\sigma(\omega) = \omega\varepsilon_0\varepsilon''(\omega) \quad (2)$$

where ε_0= permittivity of free space.

Since the 1950s, many studies have been conducted to determine the value of the dielectric properties of human tissues. Mainly two types of studies – ex-vivo and in-vivo are performed. In ex-vivo studies, tissues are separated from the body (such as breast reduction surgeries) and then studied in the lab. Whereas in the in-vivo studies the dielectric properties are determined directly in the tissue attached to the body by using tomography or by creating a dielectric map of the tissue.[3,20,29-32]

Gabriel *et al.*[33-35] conducted an extensive ex-vivo studies to determine the dielectric properties of human tissues in the frequency range of 10 to 20 GHz. Choudhary *et al.*[36] also performed ex-vivo studies on 15 patients across a range of 3 to 30 GHz and found that permittivity values of malignant tissues were 3 to 5 times higher than the normal tissues. Joines *et al.*[37] also measured the dielectric properties of malignant and normal human tissues over a range of 50 to 900 MHz frequency. They found higher value of dielectric properties in malignant tissue at all frequencies. Lazebnik *et al.*,[38] also studied dielectric properties in 155 normal, benign, and cancerous tumors obtained from cancer surgeries over a frequency range 0.5-20GHz. Fig. 7(a) shows the sample of malignant tissue used for the measurement of dielectric properties in the study. The dielectric properties of cancerous tumor were found to be much higher than the normal and benign tumor, whereas, the dielectric properties of normal and

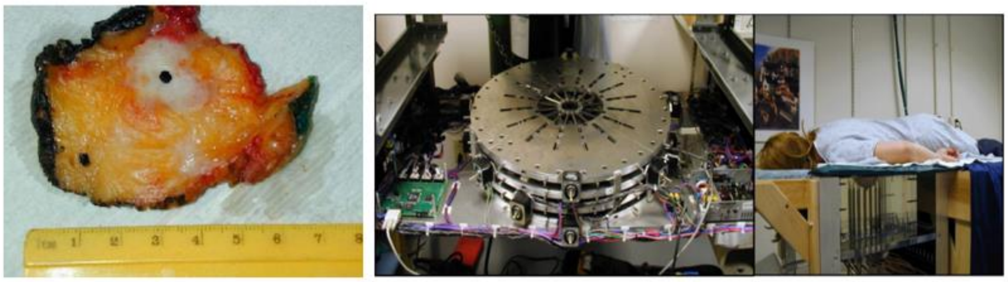

(a) (b) (c)

Fig. 7 Measuring the dielectric properties of breast tissues: (a) Ex-vivo: breast tissue specimen showing malignant tissue (white region, upper right) and normal adipose tissue (yellow region, lower left). The black ink spots mark the measurement sites. Reproduced with the permission from [38], Copyright 2007 IOP Publishing, (b) In- vivo: the Electrical Impedance Tomography (EIT) imaging system, and (c) the Microwave Tomography (MT) imaging system is positioned beneath a custom examination table during patient exams, the patient lies prone with her breast pendant through an opening in the exam table. Reproduced with the permission from [40], Copyright 2009 IOP Publishing.

benign tumors were found almost the same. Cheng *et al.*[39] also confirmed in their study that the dielectric properties of breast cancer tissues are significantly higher than the normal breast tissues.

Halter *et al.*[40] conducted both in-vivo and ex-vivo studies by performing a clinical trial on six women diagnosed with cancer. They introduced electrical impedance tomography (EIT) and microwave tomography (MT) techniques over a frequency range 10kHz to 10MHz and 0.6GHz to 1.7 GHz, respectively. Figs. 7(b) and (c) show the setup for EIT and MT imaging in an operating room, respectively. The measured properties of the breast were similar to those reported in the literature.

A study by Slanina *et al.*,[41] investigated the effect of temperature on changes in the dielectric properties. A phantom mimicking the breast was made using – distilled water, glycerin, rapeseed oil, agar, and dishwashing liquid. The phantom was heated from 25 °C to 46 °C and the dielectric properties were measured using spectroscopy. A significant contrast in the dielectric properties with respect to temperature variation was observed. Tumor exhibited the highest dielectric properties, followed by the glandular tissue, skin, and fat.

In another ex-vivo study by Nguyen *et al.*,[42] a phantom mimicking breast tissues was exposed to a high frequency antenna and the dielectric properties were measured using the S-parameter. The dielectric properties of tumor were always higher than the healthy tissues.

Table 1 shows the dielectric properties of breast tissues at 3.2 GHz frequency determined by Campbell and Land[32] in 1992. The study was conducted by performing the resonant cavity perturbation method. As can be seen there are significant differences in the dielectric properties among fatty, normal, benign, and malignant tissue.

Table 1. Dielectric properties of female breast at 3.5 GHz frequency.[32]

Tissue Type	Relative Permittivity	Conductivity (mS/cm)	Water Content (%)
Fatty tissue	2.8-7.6	0.5-2.9	11-31
Normal tissue	9.8-46	3.7-34	41-76
Benign tissue	15-67	7-49	62-84
Malignant tissue	9-59	2-34	66-79

3. Antennas used in MBI

The first ever use of antenna for breast cancer detection was proposed in early 2000s at the University of Wisconsin-Madison by Hagness *et al.*[43-47] Following that path many researchers have used different types of antennas for breast cancer detection over the years. The antenna is probably the most important part of an MI system as it is used to scan the object and collect the reflected signals, which help give essential information regarding the object. To detect the embedded tumor with high resolution, choosing an antenna that meets the requirement of MI is essential. Different types of antennas are used in different fields depending on their properties and characteristics. For the MBI system, antennas with the following characteristics are preferred.

3.1 Low profile

In MBI, we want to scan the breast tissue at multiple points to detect the tumor efficiently. For this, a low profile, light-weight, and a compact antenna is preferred. Small and portable antennas scan the tissue at smaller-smaller positions collecting more data, and hence increasing the chances of better detection. It is also an advantage if the antenna has a simple design and low manufacturing cost. An example of a low-profile antenna is the patch antenna.[48-50]

3.2 High gain

A high gain antenna radiates in a more focused direction. This is very beneficial for tumor detection since it has higher chances of microwaves getting incident on the tumor and eventually providing a high-resolution image of the breast tissues. High gain antenna also requires less power to radiate the energy making the whole system more cost-effective.[23,51]

3.3 Low reflection coefficient

The antenna should also have a low reflection coefficient in order to ensure most of its power is radiated out and not reflected back. The radiated power then incident on the breast tissues and interacts with them. More incident power increases the chances of tumor detection and provides a more detailed image of the breast.[22]

3.4 Specific absorption rate (SAR)

SAR is a measure of absorbed EM energy in the tissue. According to International Corporation of Non-Ionizing Radiation (ICNIRP) SAR in a 10gram tissue should be less than 2W/kg. Hence, it is important to measure the SAR value in the breast tissue when exposed to the antenna to ensure that the antenna is safe for use in MBI system.[52-54]

3.5 Broad frequency range

An UWB antenna is preferred for MI as it provides scanning over a wider frequency range, resulting in better contrast images between different types of tissues. The Federal Communications Commission (FCC) has set a frequency range of 3.1 GHz to 10.6 GHz for UWB devices used in microwave imaging systems.[55,56] Therefore, UWB antennas are used for MBI or are modified to ensure their bandwidth lies within the FCC guidelines.[3,10,21,57]

In MBI, a transmitter antenna is required to transmit the signals towards the breast, and a receiver antenna is needed to receive the reflected signals from the breast. Based on the number of antennas used, the MI system is categorized into three types: Monostatic imaging system– when a single antenna functions as both a transmitter and a receiver; Bi-static imaging system- when two antennas are used, one working as a transmitter and the other as a receiver; Multi-static imaging system - when an array of antenna is used in the system, with one antenna working as a transmitter at a time while the rest function as receivers. Monostatic imaging system are cheaper as they require single antenna, however, the quality of the generated images can sometimes be compromised.[58,59]

Over the years, different types of antennas such as Vivaldi, monopole, metamaterial, and patch antennas have been used in MBI system.[60-63] Almost all antennas are modified to meet the requirement of MI through parametric analysis, which includes varying the size of the radiator, varying the sizes of the slots made on the antenna, adding parasitic elements on the antenna *etc*.[63-65]

Niranjan *et al.*[66] designed a UWB miniaturized patch antenna. The slots were created in the antenna for enhancing its performance. The sizes of the slots were selected after performing the parametric analysis. It was found that after adding the slots, the antenna achieved a maximum gain of 6.43dBi and frequency range of 3.22 to 11.92 GHz. The results in this study were simulation based, no fabrication was attempted, and the simulated antenna was not tested against any breast model.

Islam *et al.*,[67] used a portable and compact tapered slot antenna in a MBI system. Slots were added to the antenna to improve its performance. The size and number of the slots were decided by performing parametric analysis. Figs. 8(a-c) show the front and back view of the proposed antenna, while Fig. 8(d) and (e) show the reflection coefficient and gain, respectively, from the parametric analysis. The antenna achieved a highest gain of 9dBi and reflection coefficient -31dB. A total of nine slots were made on the front side of the antenna, resulting in enhanced electrical length and thus better reflection coefficient and gain. Fig. 8(f) shows the experimental setup of the MBI system, where a 9-element antenna array was used to irradiate a heterogenous breast phantom. SAR in the phantom was not measured. The array scans the breast phantom, and the scattered signals were collected and processed using an imaging algorithm to detect the embedded tumor.

In our previous paper,[54] we designed a microstrip patch antenna for breast tumor detection. The design of the antenna was very simple; slots were added in the ground and patch of the antenna, which helped increase the overall performance. Fig. 9(a) shows the steps involved in the development of the antenna. Fig. 9(b) shows the reflection coefficient of the antenna at each development stage. Fig. 9(c) shows the maximum gain i.e., 4.5dB, and Fig. 9(d) shows the 3D radiation pattern of the antenna. The antenna was exposed to the breast model where it successfully detected the tumor. Specific absorption rate (SAR) in the breast model was also calculated and found to be below the safety levels.

Elsheakh *et al.*[68] used cotton material as a substrate for a textile antenna-based sensors in a wearable MBI system. The textile antenna was designed to be comfortable so that it can be used as a smart bra at home for women undergoing frequent

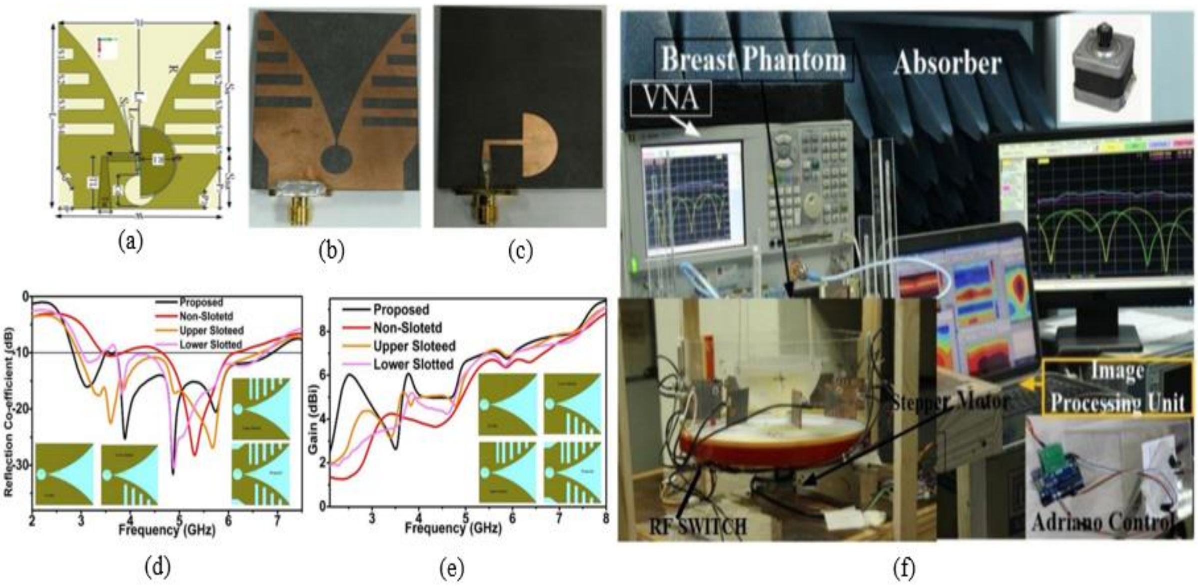

Fig. 8 (a) proposed antenna, (b) fabricated proposed antenna front view, (c) fabricated proposed antenna back view, (d)return loss (e) gain (f)experimental setup. Reproduced with the permission from [67].

scanning. Fig. 10(a) shows the design of the proposed antenna. Fig. 10(b) shows the fabricated antenna connected to a VNA. The antenna achieved a maximum gain of 3dBi and return loss -29dB. The antenna was also measured for SAR, and the resultant values came under the threshold value to cause any harmful effect. The antenna scans a breast phantom in both tumor-present and tumor-absent scenarios. Fig. 10(c) shows a monostatic imaging setup, whereas Fig. 10(d) shows the bi-static imaging setup. Return loss values for S11 and S12 were measured in 3 cases: in breast, tumor, and tumor inside breast. As shown in Fig. 10 (e) and (f), the return loss values show variations in the presence and absence of the tumor. The system showed a promising future in providing a safe, cheaper, and at home monitoring for breast cancer detection.

Hossain *et al.*,[69] designed a UWB planar antenna with a semicircular patch and a ground plane in shape of a trapezoidal. Figs. 11(a-c) shows the evolution of the proposed antenna, and Figs. 11(d) and (e) show the return loss and gain, respectively, for each evolution step of the antenna. As can be seen the proposed design of the antenna has better performance. The proposed antenna operates between 2.30 to 11 GHz with a gain of 5.80 dBi. The antenna was also fabricated and validated with the simulated results. Figs. 11(f) and (g) shows the measurement setup for the fabricated antennas. Later, a 16

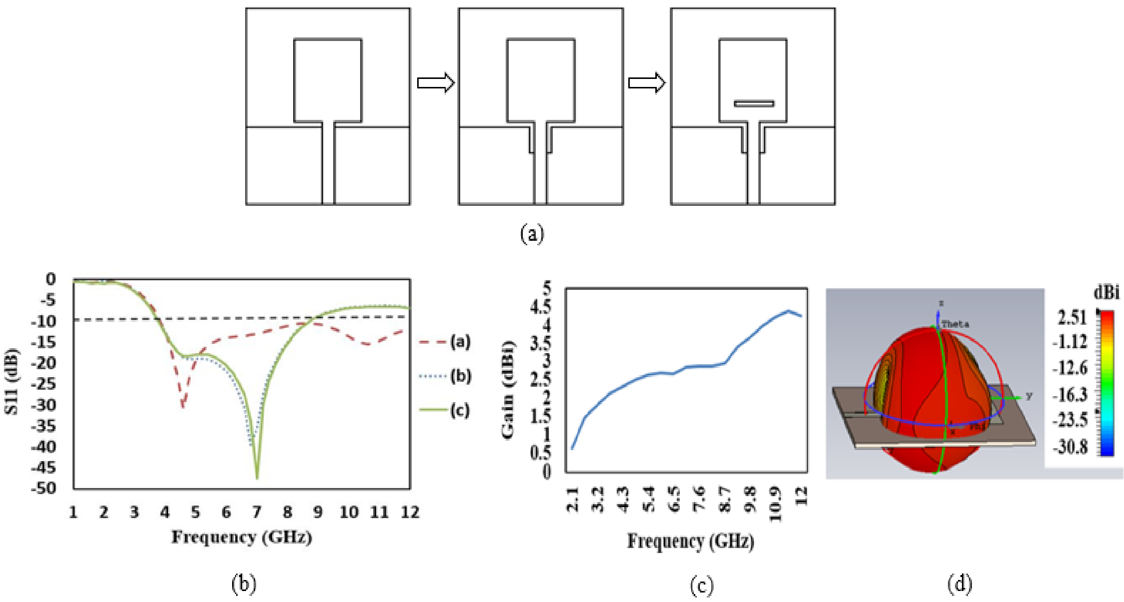

Fig. 9 (a) Development of antenna model, (b) S11 (reflection coefficient), (c) maximum gain of antenna, (d) 3D radiation pattern of antenna at 7GHz. Reproduced with the permission from [54].

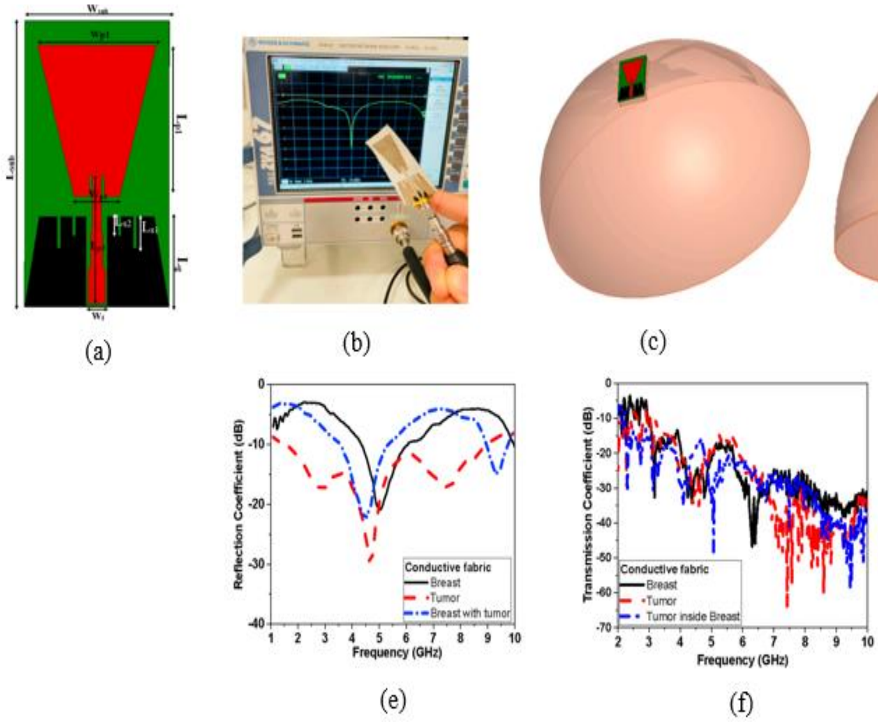

Fig. 10 (a) design of the proposed textile antenna (b) fabricated antenna connected to VNA, (c) breast phantom scanning with one antenna, (d) breast phantom scanning with two antennas, (e)measured S11, and (f) measured S21. Reproduced with the permission from [68].

element antenna array setup was designed using the simulation where a breast phantom was exposed to the antenna array, shown in Figs. 11(h). The antenna array was able to detect the tumor. A 2D image of the breast showing the tumor inside it was generated using the Iteratively Corrected Delay and Sum (IC–DAS) algorithm. The study did not calculate SAR for the antenna.

Table 2 summarizes more studies on the antennas for MBI. Parameters such as dimension, gain, return loss of the antennas are mentioned.

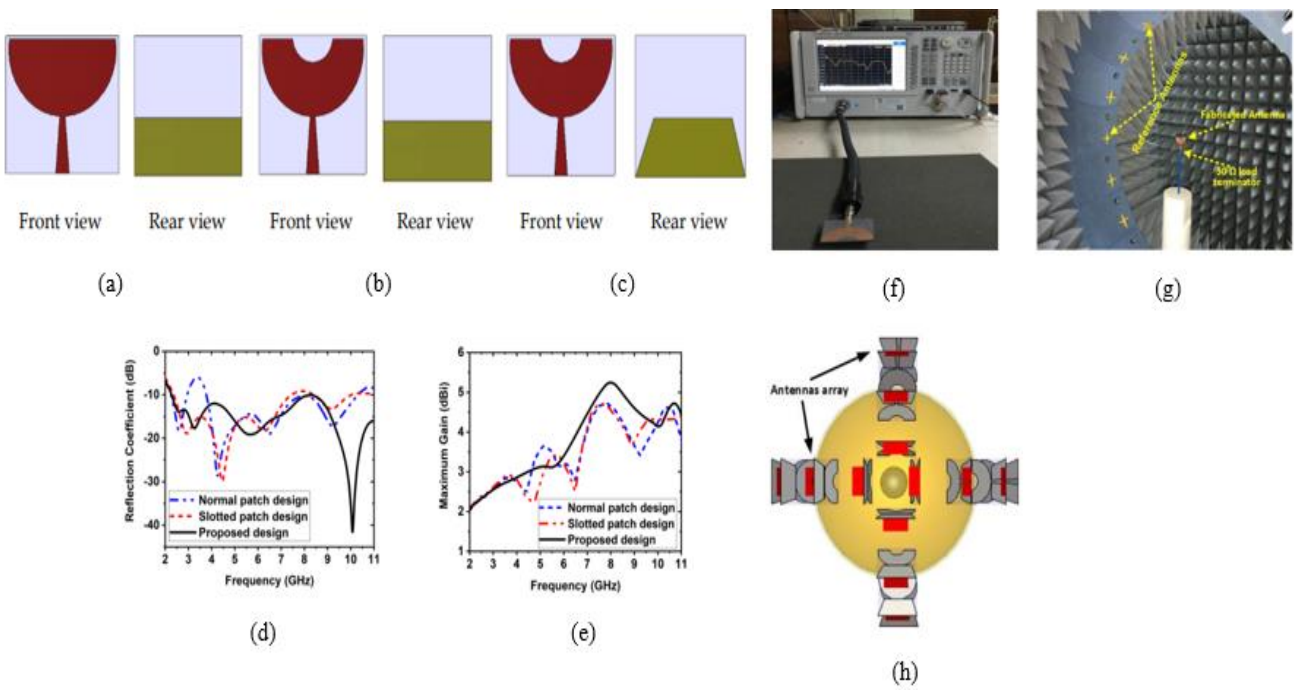

Fig. 11 (a) normal patch design, (b) slotted patch design, (c) proposed antenna, (d) S11 (reflection coefficient), (e) maximum gain, (f) PNA measurement scenario, (g) StarLab measurement scenario, and (h) 16-antenna array imaging setup. Reproduced with the permission from [69].

Table 2. Summary of antenna used for microwave breast imaging (MBI).

Ref.	Antenna	Dimensions (L×W×h) mm^3	Frequency range (GHz)	Gain	Return loss (S11)	Monostatic/bi-static/multi-static	Remark
[70]	Microstrip patch antenna	25×30×0.794	3.6 - 9.2	4.5dB	-48dB	Monostatic	-antenna simulated. -SAR calculated. -antenna exposed to breast model in simulation.
[71]	Patch antenna	34×36×1.6	2.4 - 4.7	-	-30dB	Monostatic	-antenna simulated and fabricated. -SAR not calculated. -antenna exposed to breast model in simulation and experiment.
[72]	UWB stacked coupled Microstrip patch antenna.	37×43×4.85	4.9 - 10.9	6.32dB	-30dB	Monostatic	-antenna simulated and fabricated. -SAR below threshold value. -antenna exposed to breast model in simulation and experiment.
[73]	Circularly tapered Vivaldi antenna with director (CTVAD)	48×45.7×0.8	3.1-10.6	8.25dB	-33dB	Multi-static	-antenna fabricated -SAR not calculated. -antenna exposed to breast model in simulation.
[74]	Planar circular disc monopole antenna (PCDMA)	55×40×0.15	3-10	8.4dB	-35dB	-	-antenna simulated -SAR not calculated. - not exposed to any breast model.
[75]	Bow-tie antenna array	15×15×1.57	1.2 - 7	-	-26dB	Multi-static (16 antennas)	-antenna simulated and fabricated. -SAR not calculated. -antenna exposed to breast model in experiment.
[66]	Miniaturized monopole patch antenna	30×29×(FR4)	3.22-11.92	6.43dBi	-25dB	-	- antenna simulated and fabricated. - SAR not calculated. -not exposed to breast model.
[76]	UWB fractal antenna	26×12×1.6	2.58-20.95	7.21dB	-35dB	Bistatic	- antenna simulated and fabricated. -SAR calculated. -exposed to breast model in experiment.
[77]	Inward fractal antenna	10×10×1.6	8.21	2.43dB	-40dB	Multi-static	-antenna simulated and fabricated. - SAR calculated. -exposed to breast model in simulation.
[78]	Printed log periodic antenna with metamaterials	50×40×1.6	2-5	5.5 dBi	-35dB	Multi-static	-antenna simulated and fabricated. -SAR not calculated. -exposed to breast model in simulation.

4. Tomography MBI

The basis of Microwave Tomography Imaging (MTI) are that different tissues in the body have different dielectric properties, with this quality it is possible for MTI to generate a dielectric image of the breast exposed to the microwave radiation. The first step in MTI is illuminating the breast tissue with microwave signals, called scanning. The patient lies on a table where the scanning of the breast is performed with the help of an array of antennas. As the microwave signals incident on the breast, they interact with the tissues having different dielectric properties. In the second step, the reflected signals are recorded and processed through an ill-posed algorithm

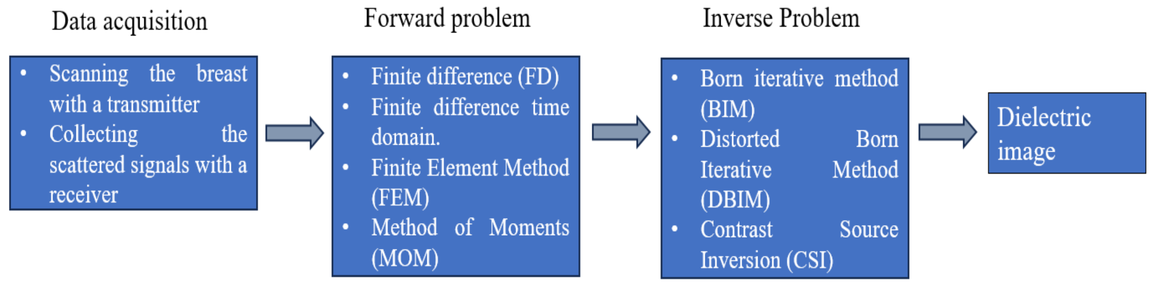

Fig. 12 Flow chart showing step-by step procedure in Tomography MBI.

(inversion algorithm) to generate 2D or 3D tomographic images of the breast based on the different dielectric properties of the tissues. The generated image is able to show the size and location of the tumor embedded in the breast.[79-81] The tomographic image has the advantage of showing the complete dielectric picture of the breast exposed to the microwave radiation, however, finding solution to the inverse problem can be challenging.[8,20,82,83]

Two types of problems are solved for reconstructing the tomographic images- forward problem and inverse problems. In forward problem, calculation of the scattered electromagnetic waves as a result of the interaction from breast layers, with known dielectric and boundary conditions, is performed.[84] That is why forward problem are highly dependent on the computational power of the problem. 3D models take significantly more time than 2D model for solving the forward problem. Some of the widely used algorithms in forward problem solving are – finite-difference (FD), finite-difference time-domain (FDTD),[43,44] finite element (FE) methods, and method of moments (MOM). In the inverse problem, reconstruction of the dielectric properties of the breast from the scattered electromagnetic fields (forward problem) is performed. Inverse problems are of two types - well-posed and ill-posed. An inverse problem is a well posed problem if it matches all three criteria - if a solution of the problem exists, the solution is unique, and the solution is continuous. If any one of these criteria is not matched the inverse problem is an ill-posed problem, which is the case for most of the times. One of the ill-posed algorithms is the Born iterative method (BIM).[85] Distorted Born Iterative Method (DBIM),[86-88] contrast source inversion (CSI).[18,89,90] *etc*. Fig. 12 shows the step-by-step procedure of Tomography MBI, starting from the scanning, to solving forward problem and inverse problem, and lastly generating the breast image.

Alibakhshikenari *et al*,[49] proposed an experimental study of detecting a breast tumor using a planar antenna- array. Total eight antennas were used in the antenna-array, each antenna has square-shaped concentric rings shown in Fig. 13(a). The antenna array radiates from 2-12 GHz, and has a gain of 4.81dB. Fig. 13(b) shows the breast phantom designed for the study, and Fig. 13(c) shows the whole experimental setup. One antenna was working as a transmitter at one time while the rest were as receivers. The collected data was in frequency domain and was converted into time domain using Inverse Fast Fourier Transform (IFFT). A Tomographic Iterative GPU-based Reconstruction (TIGRE) Toolbox was used to generate the tomographic images of the breast. Figs. 13(d-f) show the tomographic images, it was observed that in presence of the tumor, the waves were largely reflected back. The experimental setup was able to detect the presence of the tumor in the breast.

Simonov *et al.*,[91] presented a ETRI microwave imaging system for breast cancer detection. The system consists of a 16-element monopole antenna array, working at 500 MHz to 3 GHz frequency and a signal processing unit to generate 3D image of the breast, shown in Fig. 14(a). The antenna array was placed in a plastic bath filled with liquid similar to breast tissues. One antenna was working as a transmitter at one time while rest 15 were the receivers. The forward problem was solved using the FDTD method whereas the inverse problem was solved using a modified iterative Gauss-Newton method. A 40mm diameter sphere (tumor) is inserted in the bath liquid, and the antennas scan the whole bath liquid in the presence of the sphere. Figs. 14(b) and (c) shows the reconstructed tomographic images of the breast with the tumor inside it (bath liquid in presence of the sphere). The system was successful in identifying the tumor inside the healthy breast tissues.

Haynes *et al.*,[92] demonstrated a breast imaging prototype shown in Fig. 15(a). In the setup, the breast was a cavity made of 12 microwave substrates attached together, with a total 36 antennas on them (3 antennas on each substrate), shown in Fig. 15(b). One substrate (3 antennas) at one time was working as a transmitter while the rest were receivers. Both numerical and experimental analysis were performed for the breast imaging. Fig. 15(c) shows an acrylic sphere (tumor) being inserted in the breast cavity for the experimental setup. The antennas scanned the breast and an image was generated, shown in Figs. 15(d) and (e). HFSS was used to estimate the incident waves

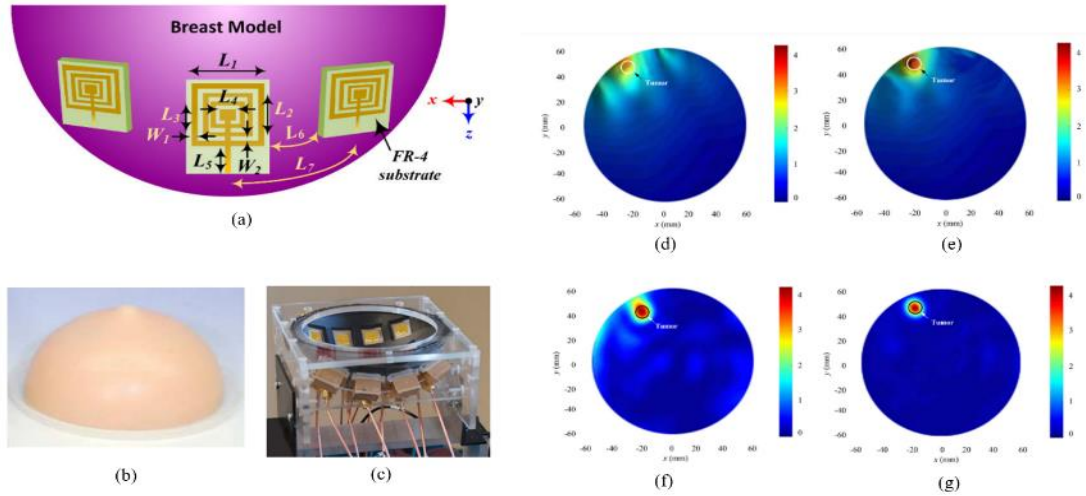

Fig. 13 (a) Side-view of antenna array arrangement around the breast, (b) breast model used in the study, (c) prototype set-up of the experimental imaging system, (d) image of tumor detection using reference antenna array using standard patches at 5.5 GHz, (e) using the proposed antenna array at 5.5 GHz, (f) using reference antenna array at 12 GHz, and (g) using the proposed antenna array at 12 GHz. Reproduced with permission from [49].

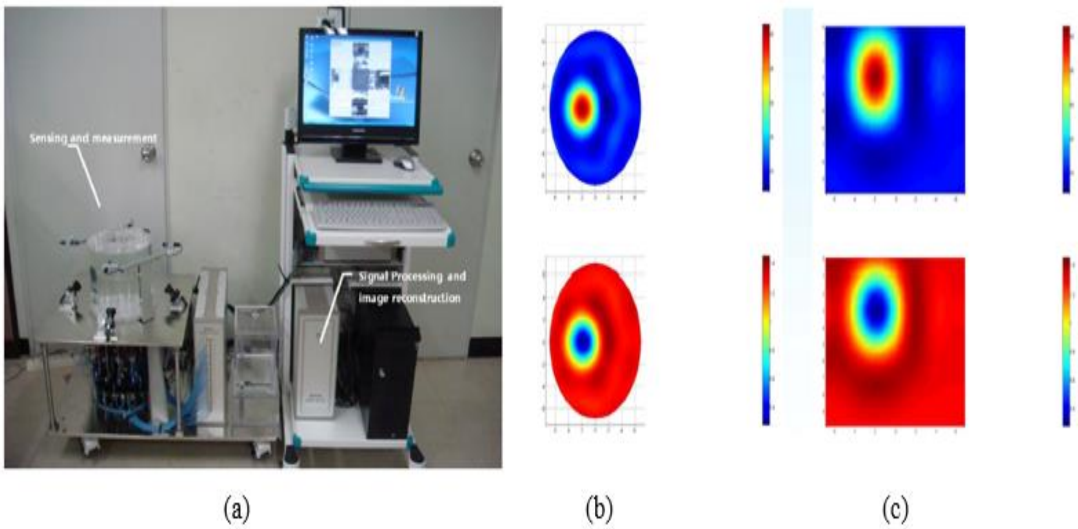

Fig. 14 (a) ETRI setup, (b) horizontal sections of the generated images, top image = permittivity, bottom image = conductivity, and (c) vertical sections of the generated images, top image = permittivity, bottom image = conductivity. Reproduced with the permission from [91].

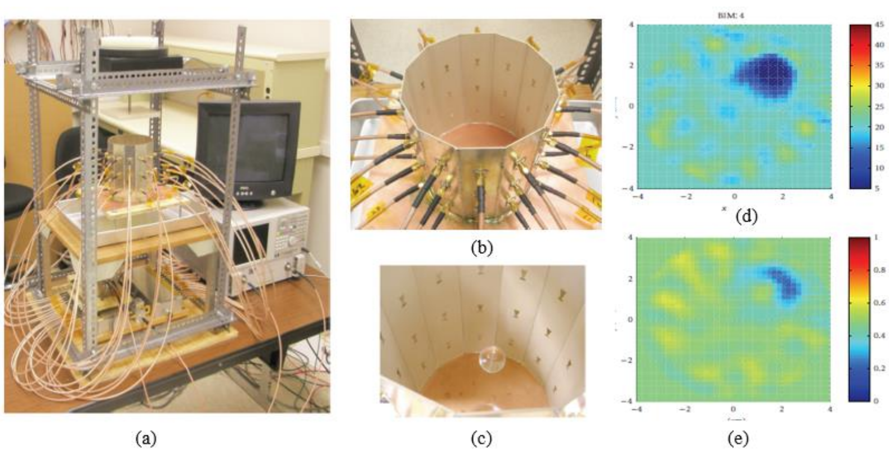

Fig. 15 (a) Breast imaging setup, (b) imaging cavity, (c) acrylic sphere suspended in the cavity, (d) reconstructed images of the breast, permittivity, (e) reconstructed images of the breast, conductivity. Reproduced with the permission from [92].

Table 3. Summary of several studies in microwave imaging of breast cancer using tomography technique.

S.no	Antenna	Type of study (clinical trial/simulation/ experimental)	Forward problem solution (software/method/setup)	Inverse problem solution (algorithms)	Discussion
[93]	32-element monopole antenna array	Clinical Trial	IBM RS6000 260 workstations, a water coupled system, Illumination tank module, and examine table.	Iterative reconstruction	5 patients were scanned for microwave imaging. The resultant permittivity images were able to detect abnormalities in tissues.
[94]	Pair of Patch antennas	Experiment and simulation	CST Microwave Studio, breast phantom, VNA, and MATLAB.	Filtered back projection (FBP)	The breast phantom was made using paraffin wax. A 10mm hole was drilled in the breast and filled with glycerin-water. The resultant image was able to detect the 10mm tumor inside the breast.
[95]	16-element monopole antenna array	Clinical	Antenna array, and FDTD	Gauss–Newton algorithm, and discrete dipole approximation	Challenges faced in hardware and software in microwave imaging were addressed and improvised. First ever 3D tomographic images of breast were presented.
[49]	8-element patch antenna array	Experiment	Breast phantom, VNA, and Finite Integration Technique (FIT).	Tomographic Iterative GPU-based Reconstruction (TIGRE) Toolbox	The proposed antenna array was able to detect the tumor inside the breast. In comparison to other antenna array in literature the proposed antennas have higher gain, small form factor.
[96]	112-monopole antennas array	Simulation and Experiment	Breast phantom, two gelatin tumor, and antenna array, and finite difference time domain (FDTD)	Soft prior and no prior	no prior and soft prior regularization techniques are compared with each other. Results show soft prior techniques are more promising in clinical trials.
[97]	32-antenna array	Experiment	glycerin – water coupling liquid (breast), low-noise amplifier, an RF amplifier, a double-balanced passive mixer, a two-stage IF amplifier, a SPDT switch, and two single-pole single-throw switches.	non-linear inverse scattering	3D images of the breast were obtained in 2 hours using the single frequency reconstruction algorithm. Malignant tissues were visible in the images.
[98]	UWB monostatic scanning	Simulation	Numerical breast phantom, FDTD, and FEM	finite element contrast source inversion (FEM-CSI).	A novel algorithm is proposed by combining MWT and radar-based region estimation. The combined algorithm shows better results than either algorithm used individually.
[99]	2GHz TM wave	Numerical and simulation	FEM	Inverse scattering problem, and single-step phase less microwave tomography.	The proposed low-cost system showed promising results for using it as a breast imaging application.

[100]	16-element circular antenna array	Clinical	FDTD	Non-linear inverse algorithm, Gauss-Newton iterative reconstruction, and MATLAB	A preclinical prototype for detection of breast cancer at Electronics and Telecommunications Research Institute (ETRI) Korea in 2010. The imaging system performs well and the obtained images are in good quality.

of the antenna on the breast and the Born Iterative Method (BIM) for generating the images of the breast. Both numerical and experimental setups succeeded in generating decent-quality breast images.

Some more studies in the tomography for MBI are discussed in Table 3.

5. Radar based MBI

Radar based MI is known to be less complex than the tomography MI. It starts with scanning the tissue just like the tomography MI. After that, the reflected signals are stored and processed through a focusing algorithm to generate an image of the tissue. This section discusses the simulations, experiments, and clinical studies in the field of radar-based microwave breast imaging.[8,12] In recent years, many radar-based MI algorithms have been developed such as – Delay-Multiply-and-Sum (DMAS), Confocal Microwave Imaging (CMI),[45] Delay and Sum (DAS),[101,102] microwave imaging via space time (MIST),[46] Generalized likelihood ratio test (GLRT), Time shift and sum, Multi-static adaptive microwave imaging (MAMI)[101] *etc*. Fig. 16 shows the steps involved in radar based MBI- Data acquisition, forward problem solving, focusing algorithms, and lastly the breast image.

In 1997, Bridges *et al.*[103] were the first to present a radar-based microwave imaging system for breast cancer detection. In their system, the breast was exposed to a generator, generating electromagnetic waves over small portions of the breast. The backscattered signals were collected and processed through a radar-based method. The system was able to detect the size and position of the tumor inside the breast due to the high contrast between a healthy and cancerous tissue.

Recently, Qashlan *et al.*[104] proposed a system where they irradiated a breast phantom using an array of nine Vivaldi antennas. The performance of the Vivaldi antenna was improved by adding slots and parasitic elements to it. The tumor detection was performed only via simulation, whereas the antenna was fabricated and measured as well. The breast phantom model was a multi layered model consisting of skin, tissue, and tumor. The breast model was exposed to the antenna array, as shown in the Fig. 17(a). The tumor detection was performed using a Microwave Radar Based Imaging Toolbox (MERIT). The system was able to detect a tumor as small as 5mm, Fig. 17(b).

Blanco-Angulo *et al.*, [105] used a 16-element Vivaldi antenna array setup for performing radar-based MI of breast cancer. The experiment includes an antenna array, breast phantom, computer, and VNA. The Vivaldi antenna was first designed in the HFSS, some modifications in the antenna were made to reduce its size and increase its performance. For the breast phantom and tumor, TRITON X- 100 (a soapy chemical compound) was used. Fig. 18 (a) shows the schematic diagram of the MI system where the antenna setup is connected to a switching network, to the PC, and then to a VNA. Fig. 18(b). shows the fabricated Vivaldi antenna array and the actual

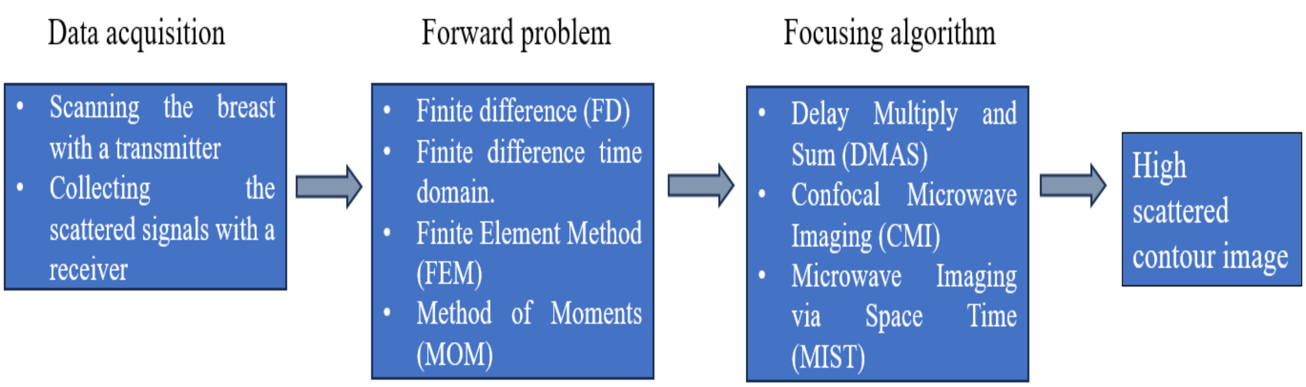

Fig. 16 Flow chart showing step-by step procedure in radar MBI.

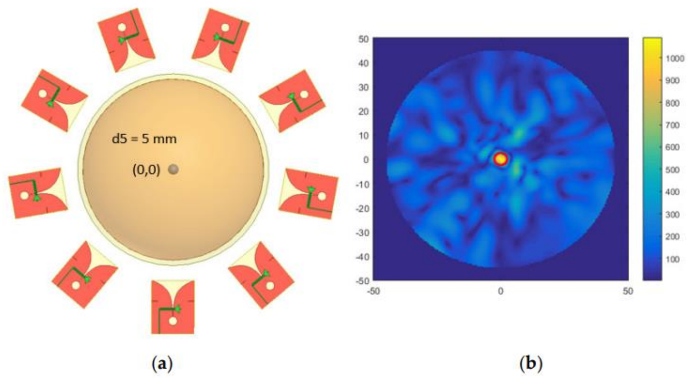

Fig. 17 Radar based MBI (a) imaging setup, (b) detected tumor. Reproduced with the permission from [104].

picture of the measurement setup of the MI system. Four different types of tumors T1-T4 having different dielectric properties were inserted in the breast and exposed to the antenna array. The Improved Delay and Sum (IDAS) imaging algorithm was used for generating the 2D images of the breast.

Figs. 18 (c-h) show the 2D image of the breast showing the tumor T1, T2, T3, and T4 inside it when the volume of the breast phantom is 1mL and 2mL.

Preece *et al.*,[102] conducted a clinical trial on 86 patients by using a series of MARIA M4 and MARIA M5 microwave imaging system. Fig. 19 shows the setup for the clinical trial, a 60- element antenna array (working between 3 to 8 GHz), was used for scanning the breast. The patients lie in prone position; breast was suspended in a ceramic cup. The system was adjusted by an operator so that the breast fits properly inside the cup and patients do not have to move at all. Delay and Sum (DAS) algorithm was used for generating the 3D images of the breast. The images were shown along the three axes: craniocaudal (CC), mediolateral, and physician point of view. The obtained images were compared with the ultrasound (US) and mammography images of the breast, as shown in Fig. 20. As can be seen, the obtained images were able to show the presence of the strongest signal with a sensitivity of >74%.

Song *et al.*,[106] conducted a clinical trial on 5 patients at Hiroshima University Hospital, Japan. The breast with invasive ductal carcinoma (IDC) and ductal carcinoma in situ (DCIS) was exposed to a hand-held impulse radar detector. The detector consists of a 16-element planar slot UWB antenna working in the range of 3.1 to 10.6 GHz frequency. SAR in the breast was also calculated by using the CST

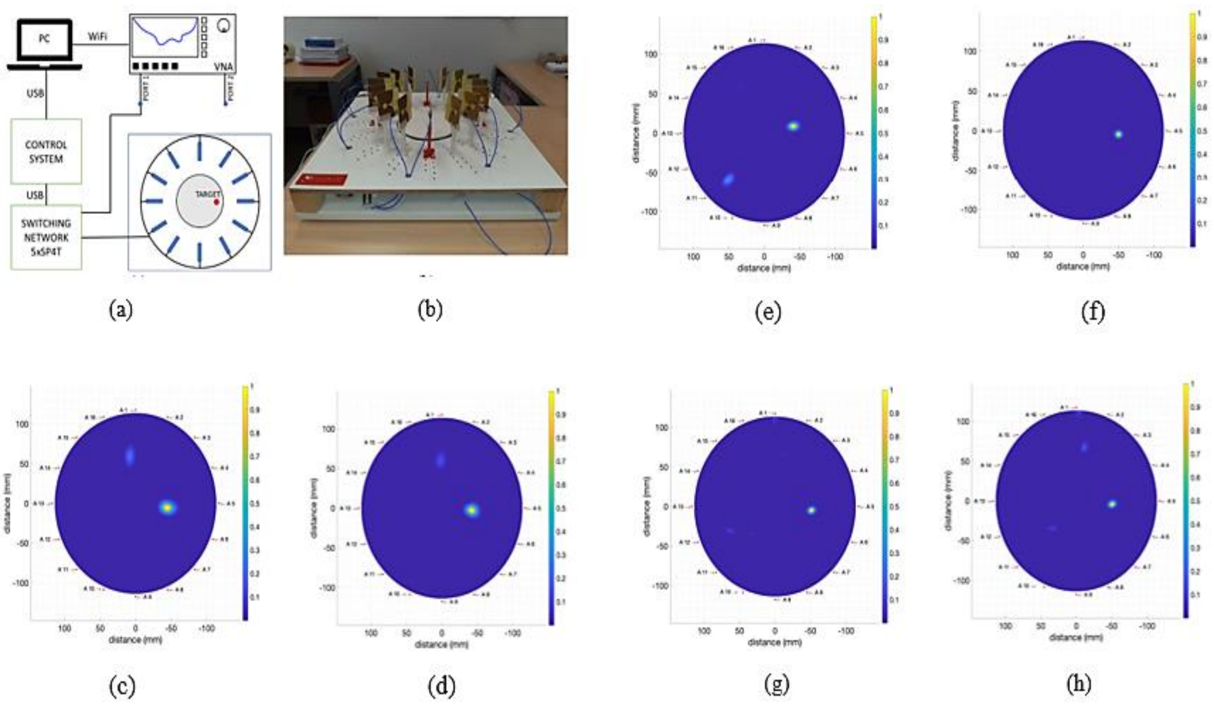

Fig. 18 (a) scheme of the proposed system, (b) picture of the measurement scenario, (c) obtained images (including breast-skin artefact removal) for the breast phantom including T1 2 mL tumor phantom; (d) T1 1 mL tumor phantom; (e) T2 2 mL tumor phantom; (f) T2 1 mL tumor phantom; (g) T3 1 mL tumor phantom; (h) T4 1 mL tumor phantom. Reproduced with the permission from [105].

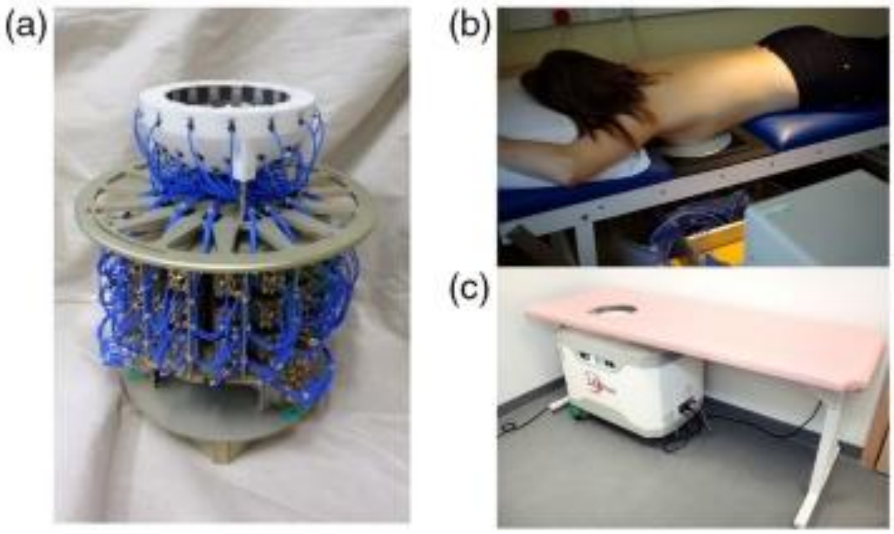

Fig. 19 MARIA M4/M5 array and bed system (a) 60 antenna array and switch assembly which moves as a unit around the breast cup, (b) MARIA M4 in position in the clinic, and (c) MARIA M5. Reproduced with the permission from [102].

software and found below the threshold value; the device was then used in the clinical trials. The patients were asked to lie down in a prone position, and the detector was placed on the breast.

Figure 21(a) shows the detector placed on a volunteer, Figs. 21(b) and (c) show the antenna dome array. Fig. 21(d) shows the pictorial diagram of the patient and the detector placed on the right breast. The scanning was performed by rotating the detector in a clockwise direction. Fig. 21(e) shows the resultant image of the breast after the scanning and Fig. 21(f) shows the 3D image of the resultant image. Fig. 21(g) is the MRI picture of the breast. The proposed system showed promising results with the MRI.

Table 4 presents more studies in the field of radar-based microwave breast imaging.

6. Clinical trials, challenges and future work in MBI

This section discusses some of the MBI machines used in clinical trials, common challenges faced in MBI techniques and ways to improve it.

Meaney *et al*[115-118] have been studying the MTI since 1990s. In 2000, they proposed the first-ever clinical prototype for MTI,[93,119] which is currently in clinical trials and showing positive results. Fig. 22(a) shows the MTI setup at the

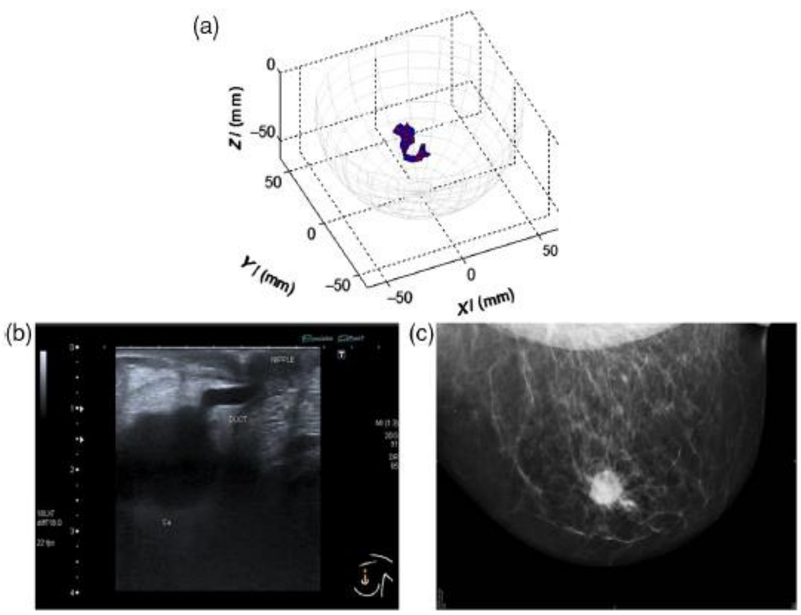

Fig. 20 An example of a MARIA scan compared with a mammogram (MMG) and ultrasound (US), (a) MARIA, (b) US scan, and (c) MMG. Only tumor is visible on mammogram. Both carcinoma and liquid-filled milk duct are visible on MARIA M4 and US scans. Reproduced with the permission from [102].

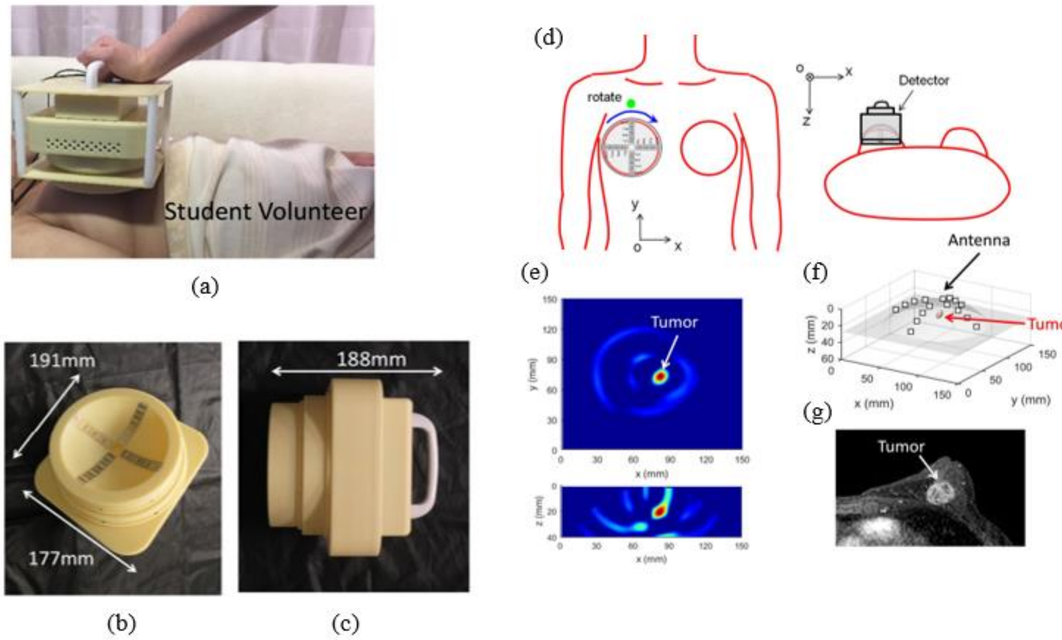

Fig. 21 (a) The hand-held microwave breast cancer detector, (b) photograph of the bottom view showing the dome antenna array, (c) photograph of the side view, (d) configuration of the clinical test for the right breast with a supine position, (e) reconstructed confocal imaging results of x-y and x-z cross sections, (f) reconstructed 3D display of the imaging area showing the location of the tumor with respect to the antenna array. (g) MRI scan of the breast. Reproduced with the permission from [106].

Table 4. Summary of several studies in radar-based microwave breast imaging.

S.no	Antenna	Type of study (clinical trial/Simulation/ experimental)	Forward problem solution (software/method/setup)	Focusing algorithm	Discussion
[104]	Array of nine Vivaldi antenna	Simulation	HFSS and Microwave Radar-based Imaging Toolbox (MERIT)	Delay-and-sum (DAS)	Antenna was simulated and fabricated. Tumor detection was performed via simulation only. Tumor of size 5mm was detected.
[43]	17-element array of monopole antenna	Simulation	FDTD	Time-shifting and coherent summing	Tumor as small as 2mm was detected
[107]	72-element omnidirectional antenna array	Simulation	FDTD	Multi-static adaptive microwave imaging (MAMI)	MAMI algorithm showed better resolution and noise reduction image of the breast in comparison to the existing algorithms.
[108]	Monostatic-Vivaldi antenna	Simulation and Experiment	CST, Breast phantom, VNA, Arduino Uno R3, L293d motor driver, and Nema11 stepper motor	DMAS	Frequency and time domain analysis was performed for the antenna. System was able to detect the tumor inside the breast and is capable to use in clinical trials.
[109]	A transceiver antenna	Simulation and Experiment	circular synthetic aperture radar (CSAR), and breast phantom.	deep neural networks (DNNs) and	The neurocomputational model in the study presents good results

				Convolutional neural networks (CNNs)	than the Matching Pursuit (MP-based) algorithms.
[59]	Monostatic – Balanced antipodal Vivaldi antenna	Clinical trial	Tissue Sensing Adaptive Radar (TSAR)	Time shift and sum	Eight patients were tested with this MI system. The system was able to detect 5mm size tumor.
[110]	Multi-static, 16-antenna array.	Experiment	A radome (inside it the breast phantom is placed), a 16-antenna array, and an oscilloscope.	Delay-Multiply-and-Sum (DMAS)	A time domain breast imaging system was able to detect tumor in a breast phantom.
[111]	31-element antenna array	Experiment	Breast phantom, antenna array, and Vector network analyzer	Delay and sum (DAS)	High resolution image of the breast was achieved by using this 31-antenna array.
[112]	16-element UWB array of antennas	Clinical and experimental	3D breast phantom for the experiment. For clinical, a healthy women's breast was scanned.	Delay and sum (DAS)	Clinical results could detect a tumor of size 8mm
[113]	16-element array of antennas	Clinical Trial	Antenna array, 13 patients, and oscilloscope.	DMAS	In this clinical trial 13 healthy patients were scanned 342 times with a time domain radar system. The aim was to determine the variability expected from the scans in the same women at different days.
[114]	60-element antenna array	Clinical Trial	Rhinoceros 3D CAD software, Fused Deposition Modelling (FDM), electromechanical switching interface, a VNA, and a hydrologic trolley.	Delay and sum (DAS)	95 patients were called on for clinical trial at the Breast Care Centre at Frenchay Hospital, Bristol. Obtained images showed good agreement when compared with the X-ray and ultrasound images. A bad fitting of breast in the ceramic cup was encountered in some cases.

Dartmouth college.[9] In their clinical study, a 16-element monopole antenna array radiating between 300MHz to 1000MHz was used. Five patients were scanned using the MTI setup. The patient lay down on the table in prone position where the breast is suspended in a tank filled with a coupling fluid of 0.9% saline. The height adjustment of the antenna array setup is controlled by computer so the patients do not have to move by themselves. One antenna acts as a transmitter at one time while the rest 15 act as receivers. The data is collected and processed through an iterative reconstruction algorithm. The system could detect abnormal tissues in the breast, including the abnormalities caused by the surgeries.

Son *et al.*[100] presented a preclinical prototype for the detection of breast cancer at Electronics and Telecommunications Research Institute (ETRI) in Korea in 2010. Fig. 22(b) shows the ETRI system where the patient lies down and the breast is suspended in an imaging bath. A 16-element circular antenna array is placed inside the matching

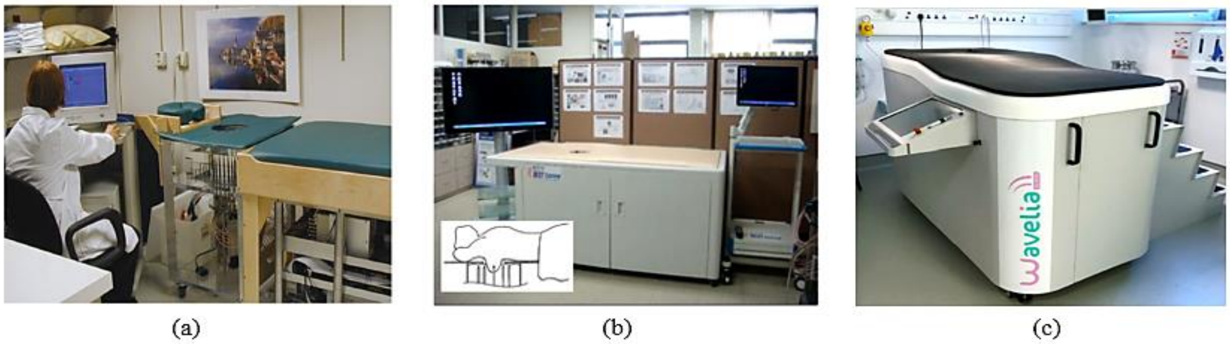

Fig. 22 (a) Microwave Tomography Imaging (MTI) system at Dartmouth College. Reproduced with the permission from [9], Copyright, 2003, IEEE. (b) Electronics and Telecommunications Research Institute (ETRI) Microwave Tomography system, Korea. Reproduced with the permission from [100] and (c) Wavelia setup in Galway University hospital, Ireland, radar-based imaging. Reproduced with the permission from [19].

bath. Each antenna radiates between 500MHz to 3GHz. The coupling liquid has the properties similar to the breast tissue. One antenna works as a transmitter at one time while the rest 15 act as receivers. Hence, a total of 240 signals are collected. The non-linear inverse algorithm is used for constructing the tomographic images. It was concluded that the imaging system performed well, detected the tumor, and successfully generated good quality images.

Another MBI system, Wavelia, was used for clinical trials from September 2018 to December 2019 at the Galway University Hospital, Ireland.[19] Total 25 women were scanned for MBI using the Wavelia system, Fig. 22(c) shows the setup. The system was able to detect the benign and cancerous tumors. However, a larger study is planned to validate the current results.

In a recent prospective clinical trial, a MammoWave microwave imaging device is tested for multicentric breast cancer detection.[120] It scans a maximum of 600 volunteers and has been certified for clinical research. Fig. 23 shows the device and a patient getting scanned. The breast images are reconstructed by using a Huygens-principle-based radar algorithm. These reconstructed images are the intensity maps of the breast based on the dielectric properties of the tissues. The whole procedure appears promising for further clinical trials.

Though MWI has many advantages over the conventional techniques (X-ray mammography, CT scan *etc*.), certain challenges have been encountered with it. However, these challenges can be addressed and resolved in future research-

6.1 Image quality

The output image of the breast from any MBI technique is the most important part of it. The quality of these images depends on many factors, such as the quality of the instruments used in the MWI system, environment, transmitted and reflected signals, algorithms used in generating the images, etc. Careful selection of such factors becomes crucial in improving the quality of the images. Also, having an experienced radiologist handle the system and interpret the images can also resolve this issue.

6.2 Comfort

MBI is a comfortable technique since it is a non-invasive technique, does not require breast compression, and does not cause any pain in the breast. However, it still requires patients to lie down in a prone position and the breast to be immersed

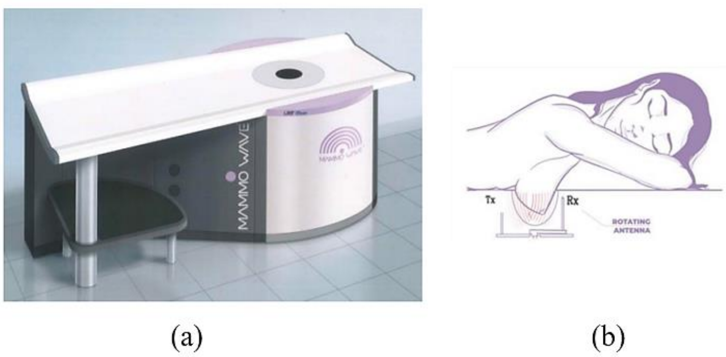

Fig. 23 (a) MammoWave device, and (b) sketch of a women laying down on the device, breast in the cup, transmitting and receiving antennas scanning the breast. Reproduced with the permission from [120].

in a liquid chamber. It is sometimes uncomfortable for some people to lay down in such position. It would be better if MBI offers more than one position for screening such as standing or sitting screening, so that patients with physical limitations feel comfortable.

6.3 Cost

MBI is known to be a cheaper alternative to the conventional methods. However, it is not always the case, it can still be expensive for the manufacturers based upon the prices of the instruments, switching circuits, antennas *etc*. used in the MBI system. Hence, switching to the devices that are cheaper but do not compromise with the output of the imaging can make the overall system cost-effective.

6.4 Combination imaging

Using MBI technique along with the conventional techniques (mammography or ultrasound) may provide better results and improve the imaging accuracy.

6.5 Clinical trials

Large scale and long-term clinical studies are needed in order to establish its benefits compared to the conventional imaging techniques.

7. Conclusion and future perspectives

Microwave imaging has been proven to be an effective alternative option to the conventional breast imaging techniques. A significant contrast in the dielectric properties of normal and cancerous tissues were reported in the literature, and used as a basis for MBI. Antennas are used to transmit and receive the microwave signal in MBI. Many research groups have performed the parametric analysis on the antennas so they meet the requirements of MBI. Some systems use a single antenna working as both a transmitter and receiver whereas some use an array of antennas (one antenna working as a transmitter while the rest are receivers). The paper discusses the state-of-the-art research in the field of active microwave imaging *i.e.* tomography and radar-based imaging. Tomography imaging is a complex method compared to radar-based imaging as it uses ill-posed algorithms to generate a dielectric image of the breast. Tomography imaging provides a full dielectric image of the breast whereas the radar-based MI only generates the image of the breast region where the tumor is located. Radar based imaging is found to be less complicated than the tomography technique.

Discussing about the future perspective of MBI, many studies are already in clinical trials and showing positive results, there are still some points that could be incorporated to make MBI the first choice for breast cancer imaging-

1. Combining the imaging algorithms- both tomography and radar-based imaging provides good result in detecting and generating the image of the embedded tumors. However, both techniques have their own disadvantages. Tomography follows a complex ill-posed complex algorithm, whereas the radar-based imaging provides limited information about the scanned tissue. A combination of both algorithms, where we could leverage the strengths of both of the techniques and mitigate the respective weakness, could be studied in the future to get a more comprehensive and detailed imaging of the breast tissues.
2. Addressing the remaining challenges- Despite the bright future of MBI, the challenges mentioned in Section 6 could be addressed to make it more affordable, efficient, and comfortable for the patients.
3. Continued development and innovation – Apart from resolving the current challenges, the future of MBI depends on innovative technology, continuous progress, and awareness among the public. Better antenna design, more comfortable systems, and increased public awareness could be the main focus in future so that it eventually becomes a preferred option for breast imaging.

Acknowledgment

This study was supported by the Thammasat Postdoctoral Fellowship (contract number TUPD6/2566), National Research Council of Thailand (Grant Number N42A650197), Thailand Science Research and Innovation Fundamental Fund (TU-FF 41/2566), and Thammasat University Research Fund (TUFT-FF20/2565).

Conflict of Interest

There is no conflict of interest.

Supporting Information

Not applicable.

References

[1] M. Arnold, E. Morgan, H. Rumgay, A. Mafra, D. Singh, M. Laversanne, J. Vignat, J. R. Gralow, F. Cardoso, S. Siesling, I. Soerjomataram, Current and future burden of breast cancer: global statistics for 2020 and 2040, *The Breast*, 2022, **66**, 15-23, doi: 10.1016/j.breast.2022.08.010.

[2] F. Bray, J. Ferlay, I. Soerjomataram, R. L. Siegel, L. A. Torre, A. Jemal, Global cancer statistics 2018: GLOBOCAN estimates of incidence and mortality worldwide for 36 cancers in 185 countries, *CA: A Cancer Journal for Clinicians*, 2018, **68**, 394-424, doi: 10.3322/caac.21492.

[3] S. Kwon, S. Lee, Recent advances in microwave imaging

for breast cancer detection, *International Journal of Biomedical Imaging*, 2016, **2016**, 5054912, doi: 10.1155/2016/5054912.
[4] J. M. Linder, A. D. Schiska, Progress in diagnosis of breast cancer: advances in radiology technology, *Asia-Pacific Journal of Oncology Nursing*, 2015, **2**, 186-191, doi: 10.4103/2347-5625.158017.
[5] J. H. Kleinknecht, A. I. Ciurea, C. A. Ciortea, Pros and cons for breast cancer screening with tomosynthesis–a review of the, *Medicine and Pharmacy Reports*, 2020, **93**, 335-341, doi: 10.15386/mpr-1698.
[6] A. B. Nover, S. Jagtap, W. Anjum, H. Yegingil, W. Y. Shih, W.-H. Shih, A. D. Brooks, Modern breast cancer detection: a technological review, *International Journal of Biomedical Imaging*, 2009, **2009**, 902326, doi: 10.1155/2009/902326.
[7] S. H. Heywang-Köbrunner, A. Hacker, S. Sedlacek, Advantages and disadvantages of mammography screening, *Breast Care*, 2011, **6**, 2, doi: 10.1159/000329005.
[8] N. AlSawaftah, S. El-Abed, S. Dhou, A. Zakaria, Microwave imaging for early breast cancer detection: current state, challenges, and future directions, *Journal of Imaging*, 2022, **8**, 123, doi: 10.3390/jimaging8050123.
[9] E. C. Fear, P. M. Meaney, M. A. Stuchly, Microwaves for breast cancer detection?, *IEEE Potentials*, 2003, **22**, 12-18, doi: 10.1109/MP.2003.1180933.
[10] S. Kwon, S. Lee, Instantaneous microwave imaging with time-domain measurements for breast cancer detection, *Electronics Letters*, 2013, **49**, 639-641, doi: 10.1049/el.2013.0248.
[11] S. Mouty, B. Bocquet, R. Ringot, N. Rocourt, P. Devos, Microwave radiometric imaging (MWI) for the characterisation of breast tumours, *The European Physical Journal Applied Physics*, 2000, **10**, 73-78, doi: 10.1051/epjap:2000121.
[12] D. Bhargava, P. Rattanadecho, Microwave imaging of breast cancer: simulation analysis of SAR and temperature in tumors for different age and type, *Case Studies in Thermal Engineering*, 2022, **31**, 101843, doi: 10.1016/j.csite.2022.101843.
[13] M. A. Aldhaeebi, K. Alzoubi, T. S. Almoneef, S. M. Bamatraf, H. Attia, O. M. Ramahi, Review of microwaves techniques for breast cancer detection, *Sensors*, 2020, **20**, 2390, doi: 10.3390/s20082390.
[14] R. A. Kruger, K. K. Kopecky, A. M. Aisen, D. R. Reinecke, G. A. Kruger, W. L. Kiser Jr, Thermoacoustic CT with radio waves: a medical imaging paradigm, *Radiology*, 1999, **211**, 275-278, doi: 10.1148/radiology.211.1.r99ap05275.
[15] L. V. Wang, X. Zhao, H. Sun, G. Ku, Microwave-induced acoustic imaging of biological tissues, *Review of Scientific Instruments*, 1999, **70**, 3744-3748, doi: 10.1063/1.1149986.
[16] Z. Wang, E. G. Lim, Y. Tang, M. Leach, Medical applications of microwave imaging, *The Scientific World Journal*, 2014, **2014**, 147016, doi: 10.1155/2014/147016.
[17] M. Xu, A. Sabouni, P. Thulasiraman, S. Noghanian, S. Pistorius, Image Reconstruction using Microwave Tomography for Breast Cancer Detection on Distributed Memory Machine, 2007 International Conference on Parallel Processing (ICPP 2007). Xi'an, China. IEEE, 2007.
[18] S. Hosseinzadegan, Fast Microwave Tomography Algorithm for Breast Cancer Imaging, Chalmers University of Technology, 2021.
[19] B. M. Moloney, P. F. McAnena, S. M. Abd Elwahab, A. Fasoula, L. Duchesne, J. D. Gil Cano, C. Glynn, A. O'Connell, R. Ennis, A. J. Lowery, M. J. Kerin, Microwave imaging in breast cancer–results from the first-In-human clinical investigation of the wavelia system, *Academic Radiology*, 2022, **29**, S211-S222, doi: 10.1016/j.acra.2021.06.012.
[20] R. Benny, T. A. Anjit, P. Mythili, An overview of microwave imaging for breast tumor detection, *Progress In Electromagnetics Research B*, 2020, **87**, 61-91, doi: 10.2528/pierb20012402.
[21] B. Borja, J. A. Tirado-Mendez, H. Jardon-Aguilar, An overview of uwb antennas for microwave imaging systems for cancer detection purposes, *Progress In Electromagnetics Research B*, 2018, **80**, 173-198, doi: 10.2528/pierb18030302.
[22] U. Rafique, S. Pisa, R. Cicchetti, O. Testa, M. Cavagnaro, Ultra-wideband antennas for biomedical imaging applications: a survey, *Sensors*, 2022, **22**, 3230, doi: 10.3390/s22093230.
[23] H. M. El Misilmani, T. Naous, S. K. Al Khatib, K. Y. Kabalan, A survey on antenna designs for breast cancer detection using microwave imaging, *IEEE Access*, 2020, **8**, 102570-102594, doi: 10.1109/ACCESS.2020.2999053.
[24] L. Wang, Microwave imaging and sensing techniques for breast cancer detection, *Micromachines*, 2023, **14**, 1462, doi: 10.3390/mi14071462.
[25] S. Di Maria, S. Vedantham, P. Vaz, Breast dosimetry in alternative X-ray-based imaging modalities used in current clinical practices, *European journal of radiology*, 2022, 155, 110509, doi: 10.1016/j.ejrad.2022.110509.
[26] Y. Kuwahara, Microwave imaging for early breast cancer detection, New Perspectives in Breast Imaging: InTech, 2017.
[27] A. C. Society, About Breast Cancer, 2024.
[28] S. Salahuddin, A. La Gioia, M. A. Elahi, E. Porter, M. O'Halloran, A. Shahzad, Comparison of *in-vivo* and *ex-vivo* dielectric properties of biological tissues, 2017 International Conference on Electromagnetics in Advanced Applications (ICEAA). Verona, Italy. IEEE, 2017.
[29] K. Sasaki, E. Porter, E. A. Rashed, L. Farrugia, G. Schmid, Measurement and image-based estimation of dielectric properties of biological tissues—past, present, and future, *Physics in Medicine & Biology*, 2022, **67**, 14TR01, doi: 10.1088/1361-6560/ac7b64.
[30] J. Cho, J. Yoon, S. Cho, K. Kwon, S. Lim, D. Kim, E. S. Lee, C. H. Kim, J. W. Choi, C. Cheon, Y. Kwon, *In-vivo* measurements of the dielectric properties of breast carcinoma xenografted on nude mice, *International Journal of Cancer*, 2006, **119**, 593-598, doi: 10.1002/ijc.21896.
[31] A. Martellosio, M. Pasian, M. Bozzi, L. Perregrini, A. Mazzanti, F. Svelto, P. E. Summers, G. Renne, L. Preda, M. Bellomi, Dielectric properties characterization from 0.5 to 50

GHz of breast cancer tissues, *IEEE Transactions on Microwave Theory and Techniques*, 2017, **65**, 998-1011, doi: 10.1109/TMTT.2016.2631162.

[32] A. M. Campbell, D. V. Land, Dielectric properties of female human breast tissue measured in vitro at 3.2 GHz, *Physics in Medicine and Biology*, 1992, **37**, 193-210, doi: 10.1088/0031-9155/37/1/014.

[33] C. Gabriel, S. Gabriel, E. Corthout, The dielectric properties of biological tissues: I. Literature survey, *Physics in Medicine and Biology*, 1996, **41**, 2231-2249, doi: 10.1088/0031-9155/41/11/001.

[34] S. Gabriel, R. W. Lau, C. Gabriel, The dielectric properties of biological tissues: II. Measurements in the frequency range 10 Hz to 20 GHz, *Physics in Medicine and Biology*, 1996, **41**, 2251-2269, doi: 10.1088/0031-9155/41/11/002.

[35] C. Gabriel, Compilation of the dielectric properties of body tissues at RF and microwave frequencies, 1996.

[36] S. S. Chaudhary, R. K. Mishra, A. Swarup, J. M. Thomas, Dielectric properties of normal & malignant human breast tissues at radiowave & microwave frequencies, *Indian Journal of Biochemistry and Biophysics*, 1984, **21**, 76-79.

[37] W. T. Joines, Y. Zhang, C. Li, R. L. Jirtle, The measured electrical properties of normal and malignant human tissues from 50 to 900 MHz, *Medical Physics*, 1994, **21**, 547-550, doi: 10.1118/1.597312.

[38] M. Lazebnik, D. Popovic, L. McCartney, C. B. Watkins, M. J. Lindstrom, J. Harter, S. Sewall, T. Ogilvie, A. Magliocco, T. M. Breslin, W. Temple, D. Mew, J. H. Booske, M. Okoniewski, S. C. Hagness, A large-scale study of the ultrawideband microwave dielectric properties of normal, benign and malignant breast tissues obtained from cancer surgeries, *Physics in Medicine and Biology*, 2007, **52**, 6093-6115, doi: 10.1088/0031-9155/52/20/002.

[39] Y. Cheng, M. Fu, Dielectric properties for non-invasive detection of normal, benign, and malignant breast tissues using microwave theories, *Thoracic Cancer*, 2018, **9**, 459-465, doi: 10.1111/1759-7714.12605.

[40] R. J. Halter, T. Zhou, P. M. Meaney, A. Hartov, R. J. Barth Jr, K. M. Rosenkranz, W. A. Wells, C. A. Kogel, A. Borsic, E. J. Rizzo, K. D. Paulsen, The correlation of *in-vivo* and *ex-vivo* tissue dielectric properties to validate electromagnetic breast imaging: initial clinical experience, *Physiological Measurement*, 2009, **30**, S121-S136, doi: 10.1088/0967-3334/30/6/s08.

[41] T. Slanina, D. H. Nguyen, J. Moll, V. Krozer, Temperature dependence studies of tissue-mimicking phantoms for ultra-wideband microwave breast tumor detection, *Biomedical Physics & Engineering Express*, 2022, **8**, 055017, doi: 10.1088/2057-1976/ac811b.

[42] D. H. Nguyen, J. Stindl, T. Slanina, J. Moll, V. Krozer, G. Zimmer, High frequency breast imaging: experimental analysis of tissue phantoms, *IEEE Open Journal of Antennas and Propagation*, 2021, **2**, 1098-1107, doi: 10.1109/OJAP.2021.3127653.

[43] S. C. Hagness, A. Taflove, J. E. Bridges, Two-dimensional FDTD analysis of a pulsed microwave confocal system for breast cancer detection: fixed-focus and antenna-array sensors, *IEEE Transactions on Biomedical Engineering*, 1998, **45**, 1470-1479, doi: 10.1109/10.730440.

[44] S. C. Hagness, A. Taflove, J. E. Bridges, Three-dimensional FDTD analysis of a pulsed microwave confocal system for breast cancer detection: design of an antenna-array element, *IEEE Transactions on Antennas and Propagation*, 1999, **47**, 783-791, doi: 10.1109/8.774131.

[45] E. C. Fear, X. Li, S. C. Hagness, M. A. Stuchly, Confocal microwave imaging for breast cancer detection: localization of tumors in three dimensions, *IEEE Transactions on Biomedical Engineering*, 2002, **49**, 812-822, doi: 10.1109/TBME.2002.800759.

[46] E. J. Bond, X. Li, S. C. Hagness, B. D. Van Veen, Microwave imaging via space-time beamforming for early detection of breast cancer, *IEEE Transactions on Antennas and Propagation*, 2003, **51**, 1690-1705, doi: 10.1109/TAP.2003.815446.

[47] X. Li, S. K. Davis, S. C. Hagness, D. W. van der Weide, B. D. Van Veen, Microwave imaging via space-time beamforming: experimental investigation of tumor detection in multilayer breast phantoms, *IEEE Transactions on Microwave Theory and Techniques*, 2004, **52**, 1856-1865, doi: 10.1109/TMTT.2004.832686.

[48] S. Ahsan, Z. Guo, I. Gouzouasis, E. Kallos, P. Kosmas, Development of a slotted triangular patch antenna for microwave tomography, 2016.

[49] M. Alibakhshikenari, B. S. Virdee, P. Shukla, N. O. Parchin, L. Azpilicueta, C. H. See, R. A. Abd-Alhameed, F. Falcone, I. Huynen, T. A. Denidni, E. Limiti, Metamaterial-inspired antenna array for application in microwave breast imaging systems for tumor detection, *IEEE Access*, 2020, **8**, 174667-174678, doi: 10.1109/access.2020.3025672.

[50] M. F. Imani, J. N. Gollub, O. Yurduseven, A. V. Diebold, M. Boyarsky, T. Fromenteze, L. Pulido-Mancera, T. Sleasman, D. R. Smith, Review of metasurface antennas for computational microwave imaging, *IEEE Transactions on Antennas and Propagation*, 2020, **68**, 1860-1875, doi: 10.1109/tap.2020.2968795.

[51] M. T. Islam, M. Samsuzzaman, S. Kibria, N. Misran, M. T. Islam, Metasurface Loaded High Gain Antenna based Microwave Imaging using Iteratively Corrected Delay Multiply and Sum Algorithm, *Scientific Reports*, 2019, **9**, 17317, doi: 10.1038/s41598-019-53857-0.

[52] A. Nazeri, A. Abdolali, M. Mehdi, An extremely safe low-SAR antenna with study of its electromagnetic biological effects on human head, *Wireless Personal Communications*, 2019, **109**, 1449-1462, doi: 10.1007/s11277-019-06621-6.

[53] A. G. Dagheyan, A. Molaei, R. Obermeier, J. Martinez-Lorenzo, Preliminary imaging results and SAR analysis of a microwave imaging system for early breast cancer detection, 2016 38th Annual International Conference of the IEEE

Engineering in Medicine and Biology Society (EMBC). Orlando, FL, USA. IEEE, 2016.
[54] D. Bhargava, P. Rattanadecho, Microstrip antenna for radar-based microwave imaging of breast cancer: simulation analysis, *International Journal on Communications Antenna and Propagation* (*IRECAP*), 2022, **12**, 47, doi: 10.15866/irecap.v12i1.20702.
[55] S. S. Ahmed, J. F. Mahdi, M. A. Kadhim, Design of ultra-wideband microwave antenna array for detection breast cancer tumours, *IOP Conference Series*: *Materials Science and Engineering*, 2020, **881**, 012112, doi: 10.1088/1757-899x/881/1/012112.
[56] R. Morey, Response to FCC 98-208 notice of inquiry in the matter of revision of part 15 of the commission's rules regarding ultra-wideband transmission systems, 1998.
[57] S. Subramanian, B. Sundarambal, D. Nirmal, Investigation on simulation-based specific absorption rate in ultra-wideband antenna for breast cancer detection, *IEEE Sensors Journal*, 2018, **18**, 10002-10009, doi: 10.1109/JSEN.2018.2875621.
[58] H. Jumaat, M. T. Ali, K. H. Ping, N. M. Faudzi, N. Miswadi, H. Yon, A review of frequency selection and antenna arrangement system for microwave imaging in early breast cancer detection, *Journal of Physics*: *Conference Series*, 2019, **1372**, 012004, doi: 10.1088/1742-6596/1372/1/012004.
[59] E. C. Fear, J. Bourqui, C. Curtis, D. Mew, B. Docktor, C. Romano, Microwave breast imaging with a monostatic radar-based system: a study of application to patients, *IEEE Transactions on Microwave Theory and Techniques*, 2013, **61**, 2119-2128, doi: 10.1109/TMTT.2013.2255884.
[60] B. J. Mohammed, A. M. Abbosh, D. Ireland, M. E. Bialkowski, Compact wideband antenna immerssed in optimum coupling liquid for microwave imaging of brain stroke, *Progress In Electromagnetics Research C*, 2012, **27**, 27-39, doi: 10.2528/PIERC11102708.
[61] N. Ojaroudi, M. Ojaroudi, A novel design of microstrip antenna for microwave imaging application, *Microwave and Optical Technology Letters*, 2013, **55**, 1755-1758, doi: 10.1002/mop.27680.
[62] T. Sugitani, S. Kubota, A. Toya, X. Xiao, T. Kikkawa, A compact 4 $\times$ 4 planar UWB antenna array for 3-D breast cancer detection, *IEEE Antennas and Wireless Propagation Letters*, 2013, **12**, 733-736, doi: 10.1109/LAWP.2013.2270933.
[63] A. Martínez-Lozano, C. Blanco-Angulo, H. García-Martínez, R. Gutiérrez-Mazón, G. Torregrosa-Penalva, E. Ávila-Navarro, J. M. Sabater-Navarro, UWB-printed rectangular-based monopole antenna for biological tissue analysis, *Electronics*, 2021, **10**, 304, doi: 10.3390/electronics10030304.
[64] A. Hossain, M. T. Islam, A. F. Almutairi, M. S. J. Singh, K. Mat, M. Samsuzzaman, An octagonal ring-shaped parasitic resonator based compact ultrawideband antenna for microwave imaging applications, *Sensors*, 2020, **20**, 1354, doi: 10.3390/s20051354.
[65] M. Z. Mahmud, M. T. Islam, A. F. Almutairi, M. Samsuzzaman, U. K. Acharjee, M. T. Islam, A parasitic resonator-based diamond-shaped microstrip antenna for microwave imaging applications, *Electronics*, 2019, **8**, 434, doi: 10.3390/electronics8040434.
[66] N. Niranjan kumar, B. S. Srikanth, S. B. Gurung, S. Manu, G. N. S. Gowthami, T. Ali, S. Pathan, A slotted UWB monopole antenna with truncated ground plane for breast cancer detection, *Alexandria Engineering Journal*, 2020, **59**, 3767-3780, doi: 10.1016/j.aej.2020.06.034.
[67] M. T. Islam, M. Z. Mahmud, M. T. Islam, S. Kibria, M. Samsuzzaman, A Low Cost and Portable Microwave Imaging System for Breast Tumor Detection Using UWB Directional Antenna array, *Scientific Reports*, 2019, **9**, 15491, doi: 10.1038/s41598-019-51620-z.
[68] D. N. Elsheakh, R. A. Mohamed, O. M. Fahmy, K. Ezzat, A. R. Eldamak, Complete breast cancer detection and monitoring system by using microwave textile based antenna sensors, *Biosensors*, 2023, **13**, 87, doi: 10.3390/bios13010087.
[69] A. Hossain, M. T. Islam, M. T. Islam, M. E. H. Chowdhury, H. Rmili, M. Samsuzzaman, A planar ultrawideband patch antenna array for microwave breast tumor detection, *Materials*, 2020, **13**, 4918, doi: 10.3390/ma13214918.
[70] D. Bhargava, P. Rattanadecho, Microstrip antenna for radar-based microwave imaging of breast cancer: simulation analysis, *International Journal on Communications Antenna and Propagation* (*IRECAP*), 2022, **12**, 47, doi: 10.15866/irecap.v12i1.20702.
[71] V. Selvaraj, D. Baskaran, P. H. Rao, P. Srinivasan, R. Krishnan, Breast tissue tumor analysis using wideband antenna and microwave scattering, *IETE Journal of Research*, 2021, **67**, 49-59, doi: 10.1080/03772063.2018.1531067.
[72] G. Kaur, A. Kaur, Breast tissue tumor detection using "*S*" parameter analysis with an UWB stacked aperture coupled microstrip patch antenna having a "+" shaped defected ground structure, *International Journal of Microwave and Wireless Technologies*, 2020, **12**, 635-651, doi: 10.1017/s1759078719001442.
[73] S. Guruswamy, R. Chinniah, K. Thangavelu, Design and implementation of compact ultra-wideband Vivaldi antenna with directors for microwave-based imaging of breast cancer, *Analog Integrated Circuits and Signal Processing*, 2021, **108**, 45-57, doi: 10.1007/s10470-021-01859-2.
[74] A. R. Celik, M. B. Kurt, Development of an ultra-wideband, stable and high-directive monopole disc antenna for radar-based microwave imaging of breast cancer, *Journal of Microwave Power and Electromagnetic Energy*, 2018, **52**, 75-93, doi: 10.1080/08327823.2018.1458692.
[75] M. Jalilvand, X. Li, L. Zwirello, T. Zwick, Ultra wideband compact near-field imaging system for breast cancer detection, *IET Microwaves, Antennas & Propagation*, 2015, **9**, 1009-1014, doi: 10.1049/iet-map.2014.0735.
[76] H. T. Sediq, J. Nourinia, C. Ghobadi, B. Mohammadi, A novel shaped ultrawideband fractal antenna for medical

purposes, *Biomedical Signal Processing and Control*, 2023, **80**, 104363, doi: 10.1016/j.bspc.2022.104363.
[77] M. N. Moussa, M. A. Madi, K. Y. Kabalan, Breast tumor detection, sizing and localization using a 24-element antenna array, *IEEE Journal of Biomedical and Health Informatics*, 2022, **26**, 5109-5121, doi: 10.1109/JBHI.2022.3189640.
[78] A. Syed, M. Sheikh, M. T. Islam, H. Rmili, Metamaterial-loaded 16-printed log periodic antenna array for microwave imaging of breast tumor detection, *International Journal of Antennas and Propagation*, 2022, **2022**, 4086499, doi: 10.1155/2022/4086499.
[79] P. M. Meaney, M. W. Fanning, R. M. di Florio-Alexander, P. A. Kaufman, S. D. Geimer, T. Zhou, K. D. Paulsen, Microwave tomography in the context of complex breast cancer imaging, *Annual International Conference of the IEEE Engineering in Medicine & Biology Society*, 2010, **2010**, 3398-3401, doi: 10.1109/iembs.2010.5627932.
[80] R. C. Conceição, J. J. Mohr, M. O'Halloran, An introduction to microwave imaging for breast cancer detection, Springer, 2016.
[81] D. Gibbins, D. Byrne, T. Henriksson, B. Monsalve, I. J. Craddock, Less becomes more for microwave imaging: design and validation of an ultrawide-band measurement array, *IEEE Antennas and Propagation Magazine*, 2017, **59**, 72-85, doi: 10.1109/MAP.2017.2731198.
[82] G. Bindu, S. J. Abraham, A. Lonappan, V. Thomas, C. K. Aanandan, K. T. Mathew, Active microwave imaging for breast cancer detection, *Progress In Electromagnetics Research*, 2006, **58**, 149-169, doi: 10.2528/pier05081802.
[83] A. Fedeli, M. Maffongelli, R. Monleone, C. Pagnamenta, M. Pastorino, S. Poretti, A. Randazzo, A. Salvadè, A tomograph prototype for quantitative microwave imaging: preliminary experimental results, *Journal of Imaging*, 2018, **4**, 139, doi: 10.3390/jimaging4120139.
[84] T. Wu, R. H. Moore, E. A. Rafferty, D. B. Kopans, A comparison of reconstruction algorithms for breast tomosynthesis, *Medical Physics*, 2004, **31**, 2636-2647, doi: 10.1118/1.1786692.
[85] D. Ireland, K. Bialkowski, A. Abbosh, Microwave imaging for brain stroke detection using Born iterative method, *IET Microwaves, Antennas & Propagation*, 2013, **7**, 909-915, doi: 10.1049/iet-map.2013.0054.
[86] M. J. Burfeindt, J. D. Shea, B. D. Van Veen, S. C. Hagness, Beamforming-enhanced inverse scattering for microwave breast imaging, *IEEE Transactions on Antennas and Propagation*, 2014, **62**, 5126-5132, doi: 10.1109/TAP.2014.2344096.
[87] X. Ye, X. Chen, Subspace-based distorted-born iterative method for solving inverse scattering problems, *IEEE Transactions on Antennas and Propagation*, 2017, **65**, 7224-7232, doi: 10.1109/TAP.2017.2766658.
[88] R. Palmeri, M. T. Bevacqua, L. Crocco, T. Isernia, L. Di Donato, Microwave imaging via distorted iterated virtual experiments, *IEEE Transactions on Antennas and Propagation*, 2017, **65**, 829-838, doi: 10.1109/TAP.2016.2633070.
[89] P. M. van den Berg, R. E. Kleinman, A contrast source inversion method, *Inverse Problems*, 1997, **13**, 1607-1620, doi: 10.1088/0266-5611/13/6/013.
[90] P. M. van den Berg, Chapter 1.3.3 - Nonlinear Scalar Inverse Scattering: Algorithms and Applications, Scattering Academic Press, London, 2002.
[91] N. A. Simonov, S. I. Jeon, S. H. Son, J. M. Lee, H. J. Kim, 3D microwave breast imaging based on multistatic radar concept system, 2011 3rd International Asia-Pacific Conference on Synthetic Aperture Radar (APSAR), 2011.
[92] M. Haynes, J. Stang, M. Moghaddam, Microwave breast imaging system prototype with integrated numerical characterization, *International Journal of Biomedical Imaging*, 2012, **2012**, 706365, doi: 10.1155/2012/706365.
[93] P. M. Meaney, M. W. Fanning, D. Li, S. P. Poplack, K. D. Paulsen, A clinical prototype for active microwave imaging of the breast, *IEEE Transactions on Microwave Theory and Techniques*, 2000, **48**, 1841-1853, doi: 10.1109/22.883861.
[94] I. M. Mehedi, K. P. Rao, U. M. Al-Saggaf, H. M. Alkanfery, M. Bettayeb, R. Jannat, Intelligent tomographic microwave imaging for breast tumor localization, *Mathematical Problems in Engineering*, 2022, **2022**, 4090351, doi: 10.1155/2022/4090351.
[95] T. M. Grzegorczyk, P. M. Meaney, P. A. Kaufman, R. M. diFlorio-Alexander, K. D. Paulsen, Fast 3-D tomographic microwave imaging for breast cancer detection, *IEEE Transactions on Medical Imaging*, 2012, **31**, 1584-1592, doi: 10.1109/TMI.2012.2197218.
[96] A. H. Golnabi, P. M. Meaney, K. D. Paulsen, 3D microwave tomography of the breast using prior anatomical information, *Medical Physics*, 2016, **43**, 1933-1944, doi: 10.1118/1.4944592.
[97] V. Zhurbenko, T. Rubæk, V. Krozer, P. Meincke, Design and realisation of a microwave three-dimensional imaging system with application to breast-cancer detection, *IET Microwaves, Antennas & Propagation*, 2010, **4**, 2200, doi: 10.1049/iet-map.2010.0106.
[98] A. Baran, D. J. Kurrant, A. Zakaria, E. C. Fear, J. LoVetri, Breast imaging using microwave tomography with radar-based tissue-regions estimation, *Progress In Electromagnetics Research*, 2014, **149**, 161-171, doi: 10.2528/pier14080606.
[99] S. Costanzo, G. Lopez, Phaseless microwave tomography assessment for breast imaging: preliminary results, *International Journal of Antennas and Propagation*, 2020, **2020**, 5780243, doi: 10.1155/2020/5780243.
[100] S.-H. Son, Preclinical prototype development of a microwave tomography system for breast cancer detection, *ETRI Journal*, 2010, **32**, 901-910, doi: 10.4218/etrij.10.0109.0626.
[101] M. Klemm, I. J. Craddock, J. A. Leendertz, A. Preece, R. Benjamin, Radar-based breast cancer detection using a hemispherical antenna array—experimental results, *IEEE*

Transactions on Antennas and Propagation, 2009, **57**, 1692-1704, doi: 10.1109/TAP.2009.2019856.
[102] A. W. Preece, I. Craddock, M. Shere, L. Jones, H. L. Winton, MARIA M4: clinical evaluation of a prototype ultrawideband radar scanner for breast cancer detection, *Journal of Medical Imaging*, 2016, **3**, 033502, doi: 10.1117/1.JMI.3.3.033502.
[103] J. E. Bridges, Non-invasive system for breast cancer detection, U.S. Patent 5, 704, 355, 1998.
[104] A. M. Qashlan, R. W. Aldhaheri, K. H. Alharbi, A modified compact flexible Vivaldi antenna array design for microwave breast cancer detection, *Applied Sciences*, 2022, **12**, 4908, doi: 10.3390/app12104908.
[105] C. Blanco-Angulo, A. Martínez-Lozano, R. Gutiérrez-Mazón, C. G. Juan, H. García-Martínez, J. Arias-Rodríguez, J. M. Sabater-Navarro, E. Ávila-Navarro, Non-invasive microwave-based imaging system for early detection of breast tumors, *Biosensors*, 2022, **12**, 752, doi: 10.3390/bios12090752.
[106] H. Song, S. Sasada, T. Kadoya, M. Okada, K. Arihiro, X. Xiao, T. Kikkawa, Detectability of breast tumor by a hand-held impulse-radar detector: performance evaluation and pilot clinical study, *Scientific Reports*, 2017, **7**, 16353, doi: 10.1038/s41598-017-16617-6.
[107] Y. Xie, B. Guo, L. Xu, J. Li, P. Stoica, Multistatic adaptive microwave imaging for early breast cancer detection, *IEEE Transactions on Biomedical Engineering*, 2006, **53**, 1647-1657, doi: 10.1109/TBME.2006.878058.
[108] H. Ozmen, M. B. Kurt, Radar-based microwave breast cancer detection system with a high-performance ultrawide band antipodal Vivaldi antenna, Turkish Journal of Electrical Engineering and Computer Sciences, 2021.
[109] M. B. Bicer, Radar-based microwave breast imaging using neurocomputational models, *Diagnostics,* 2023, **13**, 930, doi: 10.3390/diagnostics13050930.
[110] E. Porter, E. Kirshin, A. Santorelli, M. Coates, M. Popović, Time-domain multistatic radar system for microwave breast screening, *IEEE Antennas and Wireless Propagation Letters*, 2013, **12**, 229-232, doi: 10.1109/LAWP.2013.2247374.
[111] M. Klemm, J. A. Leendertz, D. Gibbins, I. J. Craddock, A. Preece, R. Benjamin, Microwave radar-based differential breast cancer imaging: imaging in homogeneous breast phantoms and low contrast scenarios, *IEEE Transactions on Antennas and Propagation*, 2010, **58**, 2337-2344, doi: 10.1109/TAP.2010.2048860.
[112] M. Klemm, I. Craddock, J. Leendertz, A. Preece, R. Benjamin, Experimental and clinical results of breast cancer detection using UWB microwave radar, 2008 IEEE Antennas and Propagation Society International Symposium. San Diego, CA, USA. IEEE, 2008.
[113] E. Porter, M. Coates, M. Popović, An early clinical study of time-domain microwave radar for breast health monitoring, *IEEE Transactions on Biomedical Engineering*, 2016, **63**, 530-539, doi: 10.1109/TBME.2015.2465867.
[114] T. Henriksson, M. Klemm, D. Gibbins, J. Leendertz, T. Horseman, A. W. Preece, R. Benjamin, I. J. Craddock, Clinical trials of a multistatic UWB radar for breast imaging, 2011 *Loughborough Antennas & Propagation Conference. Loughborough, UK. IEEE,* 2011, 1-4, doi: 10.1109/LAPC.2011.6114004.
[115] P. M. Meaney, K. D. Paulsen, T. P. Ryan, Two-dimensional hybrid element image reconstruction for TM illumination, *IEEE Transactions on Antennas and Propagation*, 1995, **43**, 239-247, doi: 10.1109/8.371992.
[116] P. M. Meaney, K. D. Paulsen, A. Hartov, R. K. Crane, An active microwave imaging system for reconstruction of 2-D electrical property distributions, *IEEE Transactions on Biomedical Engineering*, 1995, **42**, 1017-1026, doi: 10.1109/10.464376.
[117] P. M. Meaney, K. D. Paulsen, A. Hartov, R. K. Crane, Microwave imaging for tissue assessment: initial evaluation in multitarget tissue-equivalent phantoms, *IEEE Transactions on Biomedical Engineering*, 1996, **43**, 878-890, doi: 10.1109/10.532122.
[118] P. M. Meaney, K. D. Paulsen, J. T. Chang, Near-field microwave imaging of biologically-based materials using a monopole transceiver system, *IEEE Transactions on Microwave Theory and Techniques*, 1998, **46**, 31-45, doi: 10.1109/22.654920.
[119] P. M. Meaney, M. W. Fanning, T. Zhou, A. Golnabi, S. D. Geimer, K. D. Paulsen, Clinical microwave breast imaging—2D results and the evolution to 3D, 2009 International Conference on Electromagnetics in Advanced Applications. Turin, Italy. IEEE, 2009.
[120] D. Álvarez Sánchez-Bayuela, N. Ghavami, C. Romero Castellano, A. Bigotti, M. Badia, L. Papini, G. Raspa, G. Palomba, M. Ghavami, R. Loretoni, M. Calabrese, A. Tagliafico, G. Tiberi, A multicentric, single arm, prospective, stratified clinical investigation to confirm MammoWave's ability in breast lesions detection, *Diagnostics*, 2023, **13**, 2100, doi: 10.3390/diagnostics13122100.

